Morphological, Histological and Ultrastructural Characterization of the Common Dolphin's Adrenal Glands

Paula Alonso-Almorox *, Alfonso Blanco, Ignacio Molpeceres-Diego, Raiden Grandía-Guzmán, Diego Llinás Rueda, Manuel Arbelo, Antonio Fernández *

Posted Date: 17 March 2026

doi: 10.20944/preprints202603.1321.v1

Keywords: *Delphinus delphis*; cetaceans; adrenal gland; HPA axis; adrenal morphology; ultrastructure; stress physiology; neuroendocrine system

 doi:10.20944/preprints202603.1321.v1

Article

Morphological, Histological and Ultrastructural Characterization of the Common Dolphin's Adrenal Glands

Paula Alonso-Almorox [1,2,*], Alfonso Blanco [2], Ignacio Molpeceres-Diego [1], Raiden Grandía Guzmán [1], Diego Llinás Rueda [1], Manuel Arbelo [1] and Antonio Fernández [1,*]

[1] Veterinary Histology and Pathology, Atlantic Center for Cetacean Research (CAIC), Institute of Animal Health and Food Safety (IUSA), Veterinary School, University of Las Palmas de Gran Canaria (ULPGC), Trasmontaña s/n, 35413 Arucas, Spain

[2] Department of Anatomy and Comparative Pathology and Anatomy, University of Cordoba, 14014 Cordoba, Spain

* Correspondence: paulaalonsoalmx@gmail.com

Simple Summary

The adrenal glands are small organs located near the kidneys that help control stress responses, metabolism, and many essential body functions. In dolphins and other marine mammals, hormone levels from these glands are often used to evaluate health and environmental stress. However, interpreting these signals correctly requires a clear understanding of what a healthy adrenal gland looks like in each species. For the short-beaked common dolphin, this detailed information has been lacking. In this study, we examined the adrenal glands of 55 short-beaked common dolphins (*Delphinus delphis*) stranded in the Canary Islands. We studied their overall shape, internal structure, and microscopic organization. We found that the glands follow the typical mammalian pattern but show some species-specific structural features. The proportion between the outer and inner regions of the gland changed during growth from immature to adult animals but did not differ between dolphins that died suddenly and those that died after longer illnesses. These results provide the first comprehensive structural reference for the adrenal gland in this species. This information will improve the interpretation of health assessments in stranded dolphins and support research on marine ecosystem health.

Abstract

The adrenal glands are central regulators of endocrine function and stress physiology, yet detailed species-specific anatomical baselines remain limited in cetaceans. This study provides a comprehensive gross, histological, morphometric, and ultrastructural characterization of the adrenal glands in 55 short-beaked common dolphins (*Delphinus delphis*) examined postmortem in the Canary Islands. Adrenal glands were evaluated macroscopically and microscopically, and histological corticomedullary ratios were calculated from mid-transverse sections. Associations with body length, sexual maturity, and cause-of-death category were assessed statistically. Transmission electron microscopy was performed to characterize cortical and medullary cellular ultrastructure. Adrenal weight showed a positive correlation with body length. Histological corticomedullary ratio showed no lateral asymmetry but differed significantly between sexually immature and mature individuals, indicating ontogenetic remodeling of adrenal architecture. In contrast, corticomedullary ratio did not differ significantly between adult dolphins that died from acute events and those with more progressive pathological conditions. Ultrastructural analysis identified characteristic steroidogenic cortical cells and two chromaffin cell populations in the medulla. These findings establish the first integrated anatomical baseline for the adrenal gland in *Delphinus delphis*, providing essential reference data for comparative anatomy, veterinary pathology, and interpretation of endocrine-related findings in cetaceans.

 doi:10.20944/preprints202603.1321.v1

Keywords: *Delphinus delphis*; cetaceans; adrenal gland; HPA axis; adrenal morphology; ultrastructure; stress physiology; neuroendocrine system

1. Introduction

The adrenal glands are key endocrine organs involved in the regulation of multiple physiological processes essential for mammalian homeostasis, including metabolism, cardiovascular function, immune modulation, and behavioral adaptation [1]. Through the synthesis and release of steroid hormones and catecholamines, the adrenal glands play a central role in mediating both basal regulatory mechanisms and adaptive responses to internal and external challenges [2].

These endocrine functions are tightly integrated within the neuroendocrine system, primarily through the hypothalamic–pituitary–adrenal (HPA) axis, which coordinates central and peripheral signaling pathways to regulate adrenal activity [3] . Activation of the HPA axis constitutes a fundamental component of the stress response system, enabling organisms to maintain physiological balance under changing environmental conditions [4–6]. Because of this pivotal function, adrenal hormones are widely used as biological indicators in many clinical and veterinary contexts, particularly in the assessment of endocrine activity and stress-related processes [7–9]. For this reason, in species such as cetaceans, which are increasingly recognized as sentinels of the marine ecosystem health and are exposed to a wide range of natural and anthropogenic pressures, the interpretation of adrenal-derived biomarkers has gained relevance [10–15]. However, meaningful interpretation of endocrine signals and biomarkers requires a thorough understanding of the underlying anatomical and cellular organization of the adrenal glands. Establishing detailed morphological and ultrastructural baselines is therefore a critical prerequisite for advancing physiological and pathological assessments in these species.

From a structural perspective, the adrenal glands are paired organs composed of two embryologically and functionally distinct compartments: the cortex and the medulla [16]. The adrenal cortex is classically organized into concentric zones that differ in cellular arrangement, cytoplasmic composition, and endocrine output. These zones typically include an outer zona glomerulosa, characterized by small cells arranged in rounded clusters or arches and primarily involved in mineralocorticoid production; a middle zona fasciculata, composed of larger, lipid-rich cells organized in radial cords and responsible for glucocorticoid synthesis; and an inner zona reticularis, formed by smaller cells arranged in an anastomosing network and associated with the production of androgen precursors [17,18]. The adrenal medulla, in contrast, consists of chromaffin cells derived from the neural crest, arranged in cords or clusters closely associated with a dense sinusoidal vascular network. These cells synthesize and store catecholamines, which are rapidly released into the circulation in response to neuroendocrine signaling [19]. In mammals, variations in cortical zonation, capsular organization, trabecular architecture, and cortico-medullary relationships have been documented among species, highlighting the importance of detailed anatomical descriptions for identifying both conserved structural patterns and species-specific adaptations across taxa [20–22].

In cetaceans, anatomical and histological studies of the adrenal glands have documented a combination of conserved mammalian organization and recurrent cetacean-specific traits, with interspecific variability across species [23–29]. One of the most consistently reported features in several delphinid species is cortical pseudolobulation, resulting from a thick connective tissue capsule and prominent trabeculae or septa extending into the parenchyma, with a varying degree among species and age [30].

Additional distinctive traits described in cetaceans involve both the cortico-medullary interface and medullary architecture. A conspicuous connective tissue layer separating cortex and medulla has been described in odontocetes, a feature not typically emphasized in domestic mammals or humans [26]. Within the medulla, several delphinid species, have been reported to exhibit two chromaffin cell populations with differential staining properties consistent with epinephrine- and norepinephrine-

 doi:10.20944/preprints202603.1321.v1

secreting cells [27,28]. These populations are often organized as an outer, more intensely stained "medullary band" surrounding an inner medulla composed of lighter cell aggregations.

Another characteristic reported with variable frequency across odontocete species, is the presence of medullary protrusions extending from the medulla through the cortex towards the capsule, occasionally even reaching the capsular surface in some species . Additional peculiarities, including invaginations of cortical tissue into the medulla around centrally located blood vessels; or cell aggregations within the capsule interpreted as accessory adrenal or interrenal-like tissue [26–29].

Alongside these qualitative traits, morphometric descriptors have been incorporated in some cetacean studies as complementary anatomical parameters. Cortex-to-medulla (CM) ratios have been used to assess interspecific and, in some cases, intraspecific differences [12,28,31]. These findings reveal that while different descriptive accounts exist for selected odontocetes, comprehensive species-specific baselines integrating gross morphology, detailed histology, and quantitative morphometrics remain limited, thereby constraining comparative and pathological interpretation in cetacean endocrine anatomy.

At the cellular level, ultrastructural investigations provide critical insights into adrenal gland organization by revealing subcellular features associated with steroidogenesis, catecholamine synthesis and storage, and cell–vascular interactions. Transmission electron microscopy (TEM) has been extensively applied to the study of adrenal glands in terrestrial mammals, where it has enabled detailed characterization of cortical and medullary cell types based on organelle composition, lipid content, and secretory granule morphology.

In cetaceans, however, ultrastructural information on the adrenal gland remains very limited. Available observations have focused on medullary organization in the Atlantic bottlenose dolphin (*Tursiops truncatus*), where TEM allowed the identification of distinct chromaffin cell populations associated with norepinephrine- and epinephrine-producing cells, based on differences in cytoplasmic electron density and granule morphology [27]. While these findings provided valuable insight into medullary cellular heterogeneity, ultrastructural descriptions of the adrenal cortex in cetaceans, as well as integrative characterizations encompassing both cortical and medullary compartments within a species, remain largely unexplored. The scarcity of comprehensive ultrastructural data underscores the need for TEM-based studies aimed at establishing, species-specific cellular baselines for cetacean adrenal glands, which are essential to support future comparative and pathological investigations.

Given the limited availability of integrative ultrastructural data in delphinids and the recognized need for species-specific anatomical baselines, attention to widely distributed and frequently examined species is particularly warranted. The short-beaked common dolphin (*Delphinus delphis*) is one of the most abundant odontocetes in temperate and subtropical waters and represents a species commonly assessed in veterinary and pathological contexts [32,33]. Despite its ecological relevance and frequent inclusion in stranding and necropsy programs, comprehensive morphological and ultrastructural characterizations of its adrenal glands remain lacking. In parallel with the increasing attention directed toward the stress response in marine mammals, characterization of the cetacean neuroendocrine system, particularly in relation to HPA axis regulation and stress physiology, has become progressively more relevant [34–36]. Establishing a detailed anatomical baseline for this species is therefore essential to support both comparative studies within *Delphinidae* and the accurate interpretation of pathological alterations in cetacean endocrine and stress-related research.

The aim of the present study is to provide an in-depth morphological, histological, morphometric, and ultrastructural characterization of the adrenal glands in the short beaked common dolphin. By integrating multiple levels of anatomical description, this work establishes a comprehensive reference framework for the species. The findings presented here contribute baseline data essential for veterinary histopathology and comparative studies of the cetacean neuroendocrine system.

 doi:10.20944/preprints202603.1321.v1

2. Materials and Methods

2.1. Animals

Adrenal glands were collected from 55 short-beaked common dolphins (*Delphinus delphis*) examined postmortem. All animals underwent complete post-mortem examinations performed by veterinarians from the pathology team at the Animal Health and Food Safety Institute (IUSA), Faculty of Veterinary Medicine, Universidad de Las Palmas de Gran Canaria (ULPGC), following the standardized cetacean necropsy protocol described by Kuiken and García Hartmann, with modifications routinely applied by the IUSA pathology team [37]. Only animals classified as fresh or very fresh were included in the study. Animals showing major adrenal pathological alterations (e.g., extensive necrosis or hemodynamic changes, neoplasia, or severe inflammatory lesions) were excluded to ensure that the present study reflects baseline morphological and ultrastructural characteristics of the species.

For each individual, sex, total body length, and sexual maturity status (determined by gonadal histology) were recorded. The cause of death was established based on gross and histopathological findings (e.g., infectious disease, parasitic disease, fishing interaction, degenerative processes). The complete morphometric and histomorphometric dataset for all examined individuals is provided in Supplementary Table S1.

Sampling of stranded dolphins from the Canary Islands was authorized by the Spanish Ministry for the Ecological Transition and Demographic Challenge and the Canarian Government's Environmental Department (project number PID2021-127687NB-10). A copy of the permit is provided in the Supplementary Materials.

2.2. Adrenal Gland Collection and Sampling

During necropsy, adrenal glands were identified and dissected *in situ*. Both adrenal glands were excised by sharp dissection and surrounding adipose and connective tissues were carefully removed to expose the gland surface without compromising the capsule.

Prior to fixation, each gland was weighed using a precision balance and measured macroscopically to obtain length and maximum width. Following gross examination, the glands were sectioned mid-transverse through their longitudinal axis. A central transverse section was used to assess internal architecture and to evaluate cortico-medullary organization. Subsequently, tissue samples approximately 0.5 cm in thickness were obtained from the central transverse plane for histological and ultrastructural processing.

2.3. Histochemical STUDY

For histological and histochemical analysis, adrenal tissue samples were fixed by immersion in 10% neutral-buffered formalin, routinely processed, and embedded in paraffin. Serial sections of 5 µm thickness were obtained.

Sections were stained with haematoxylin and eosin (H&E) for general morphological evaluation and with Masson's trichrome (MT) to assess connective tissue distribution and capsular architecture. Periodic acid–Schiff (PAS) and periodic acid–Schiff with diastase digestion (PAS-D) were performed to evaluate cytoplasmic glycoconjugates and basement membrane components. Grimelius silver impregnation staining was applied to highlight argyrophilic cells within the adrenal cortex and medulla.

Histological evaluation and image acquisition were performed using an Olympus BX51 light microscope equipped with a DP21 digital camera and a 0.5× adapter (Olympus Corp., Tokyo, Japan). The microscope's integrated measurement software was used for quantitative assessment of histological features.

 doi:10.20944/preprints202603.1321.v1

2.4. Morphometric Analysis

Morphometric variables were examined in relation to biological parameters including sex, total body length, and sexual maturity (determined based on gonadal histological evaluation).

Quantitative morphometric analyses were conducted at both the macroscopic (gross anatomical) and histological levels.

At necropsy, macroscopic measurements included adrenal weight (left and right) and maximal length. Absolute adrenal weight and length were analysed descriptively for each gland separately. In adult individuals, absolute adrenal measurements were summarised by sex and expressed as mean ± standard deviation (SD).

To account for inter-individual differences in body size, adrenal weight and adrenal length were additionally standardised by total body length and expressed as g/cm and cm/cm, respectively. Mean adrenal weight per individual was calculated as the average of left and right adrenal weights when both were available. Associations between mean adrenal weight and total body length were evaluated using Spearman's rank correlation coefficient. Cortical and medullary thicknesses were measured on fresh mid-transverse sections.

Histological morphometric analysis was performed on paraffin-embedded sections using the calibrated measurement tools integrated into the Olympus BX51 microscope imaging system. Measurements included cortical thickness, and medullary thickness for each gland. A histological corticomedullary ratio (CM) was calculated for each left and right gland using the formula:

$CM = (cortex_1 + cortex_2) / medulla$

$Cortex_1$ and $cortex_2$ represent the cortical thickness measured on both sides of the medulla.

To evaluate potential lateral asymmetry, paired comparisons between left and right CM values were performed using the Wilcoxon signed-rank test. These values were then averaged per individual (mean of left and right glands when both were available, or single measurement if just one gland was measured), generating a single per-individual CM value for subsequent analyses. Averaged CM values were later compared between sexually immature and sexually mature animals to assess differences in corticomedullary organization using the Wilcoxon rank-sum test.

CM values were also compared according to cause-of-death category in sexually mature individuals to explore whether corticomedullary proportions differed between animals that died following a sudden external event and those that experienced more progressive pathological processes. Two categories were established: acute cause of death (Acute COD), including animals that died as a result of fishing interaction, and non-acute cause of death (Non-acute COD), comprising individuals in which death was attributed to infectious disease, parasitic disease, or medical/degenerative organ failure, representing more prolonged or insidious pathological conditions. The subset of sexually mature individuals included in these comparative analyses is detailed in Supplementary Table S2. Differences in CM between these groups were assessed using the Wilcoxon rank-sum test.

Normally distributed variables are presented as mean ± SD, whereas non-normally distributed variables are reported as median and interquartile range (IQR).

Statistical analyses were performed in R, and significance was set at $p < 0.05$.

2.5. Ultrastructural Study (Transmission Electron Microscopy)

For ultrastructural analysis, selected adrenal tissue samples from 4 individuals (one adult male, one adult female, one juvenile male and one juvenile female) measuring approximately 2 × 5 mm and less than 1 mm in thickness were obtained from the central transverse plane of the gland. Samples were rinsed in phosphate-buffered saline (PBS) and fixed overnight at 4 °C in 2.5% glutaraldehyde prepared in 0.1 M phosphate buffer (pH 7.4).

Post-fixation was performed in 1% osmium tetroxide in the same buffer, followed by dehydration through a graded ethanol series and embedding in Araldite resin. Semi-thin sections were stained with toluidine blue for orientation, and ultra-thin sections were contrasted with uranyl acetate and lead citrate.

 doi:10.20944/preprints202603.1321.v1

Ultrastructural observations were carried out using a JEM 1400 transmission electron microscope (JEOL Ltd., Tokyo, Japan) at the Central Microscopy Research Facilities of the Universidad de Córdoba (Spain).

Morphometric analyses were performed using ImageJ (National Institutes of Health, Bethesda, MD, USA). The following parameters were assessed: mean cell diameter of cortical and medullary cells; diameter of secretory granules in chromaffin cells; and mean diameter of lipid droplets and mitochondria in cortical cells.

For each individual and cellular compartment, multiple measurements were obtained from well-preserved, non-overlapping cells in representative micrographs captured at comparable magnifications. Mean values were first calculated per individual. For the juvenile group (n = 2), measurements from both individuals were pooled to obtain group mean ± standard deviation (SD). For adult male and adult female categories (n = 1 each), values are presented as mean ± SD reflecting intra-individual variability only. All analyses were descriptive in nature.

3. Results

3.1. Gross anatomy and Morphology

In all examined individuals, the adrenal glands were identified as paired organs located within the abdominal cavity. The glands were consistently found in association with the cranial pole of each kidney and were readily distinguishable from surrounding tissues by their compact appearance and well-defined capsule (Figure 1).

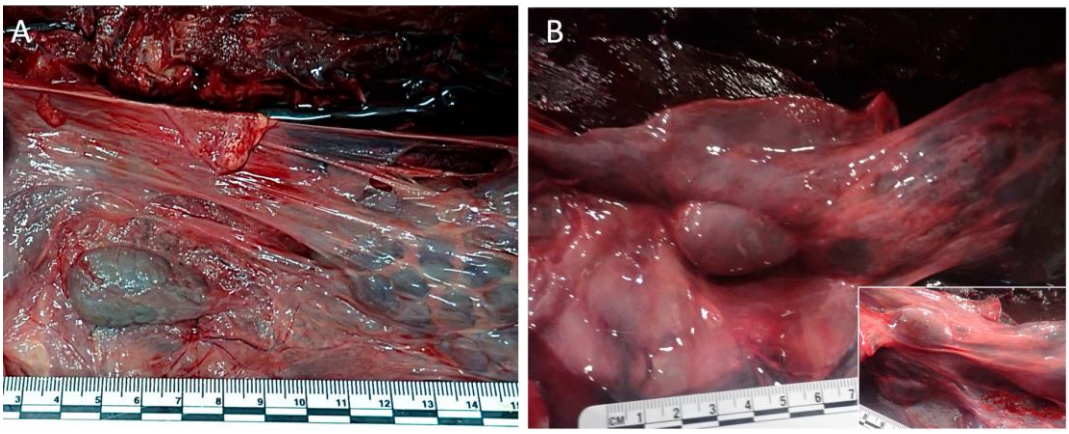

Figure 1. In situ anatomical position of the adrenal glands in *Delphinus delphis*. (A) Gross necropsy image showing the left adrenal gland located craniomedially to the cranial pole of the left kidney within the abdominal cavity. The gland is partially embedded in perirenal connective tissue. (B) Gross necropsy image of the right adrenal gland, positioned craniomedially to the right kidney and situated deeper within the perirenal tissues. Visualization requires partial reflection of the left kidney and surrounding connective tissue. The inset shows a simultaneous view of both adrenal glands in situ following bilateral exposure, illustrating their symmetrical cranial relationship to the respective kidneys and overall topographical arrangement within the abdominal cavity.

Macroscopically, the adrenal glands were generally oval to elongated in shape, with a longitudinal axis of approximately two to three times their transverse width (Figure 2). The external surface was smooth and covered by a thin but distinct fibrous capsule. A mild asymmetry between left and right glands was observed in some individuals, primarily reflected in minor differences in size and contour, with the left adrenal tending to appear more slender in many cases; however, overall gross organisation and cortico-medullary differentiation were comparable between sides.

 doi:10.20944/preprints202603.1321.v1

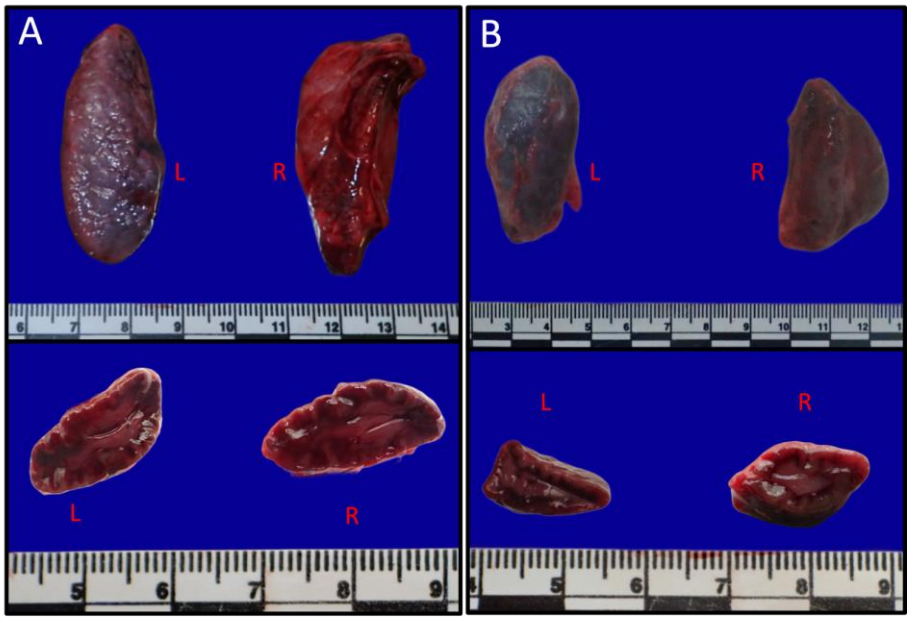

Figure 2. Gross morphology of the adrenal glands in sexually mature *Delphinus delphis***.** (A) Male adult individual. (B) Female adult individual. Upper panels show the left (L) and right (R) adrenal glands ex situ, demonstrating their elongated to oval shape. Lower panels show midtransverse sections of the corresponding glands, revealing clear cortico–medullary differentiation. The peripheral cortex appears darker in colour, whereas the centrally located medulla is lighter and more vascularised. Mild asymmetry in size and contour between left and right glands is appreciable, although overall gross organisation is comparable between sides. Scale bars in centimetres.

On the mid-transverse section, two clearly demarcated regions were evident (Figure 2). The peripheral cortex formed the outer portion of the gland and appeared darker in colour, whereas the central medulla was lighter. The cortico-medullary boundary was grossly appreciable due to darker differences in colour and texture. Prominent vascular structures were visible within the medulla's border on cut surface.

3.2. Histological Organization

Histological examination of the adrenal glands revealed a general organisation into an external capsule, a cortical component composed of three zones, and a central medulla (Figure 3).

 doi:10.20944/preprints202603.1321.v1

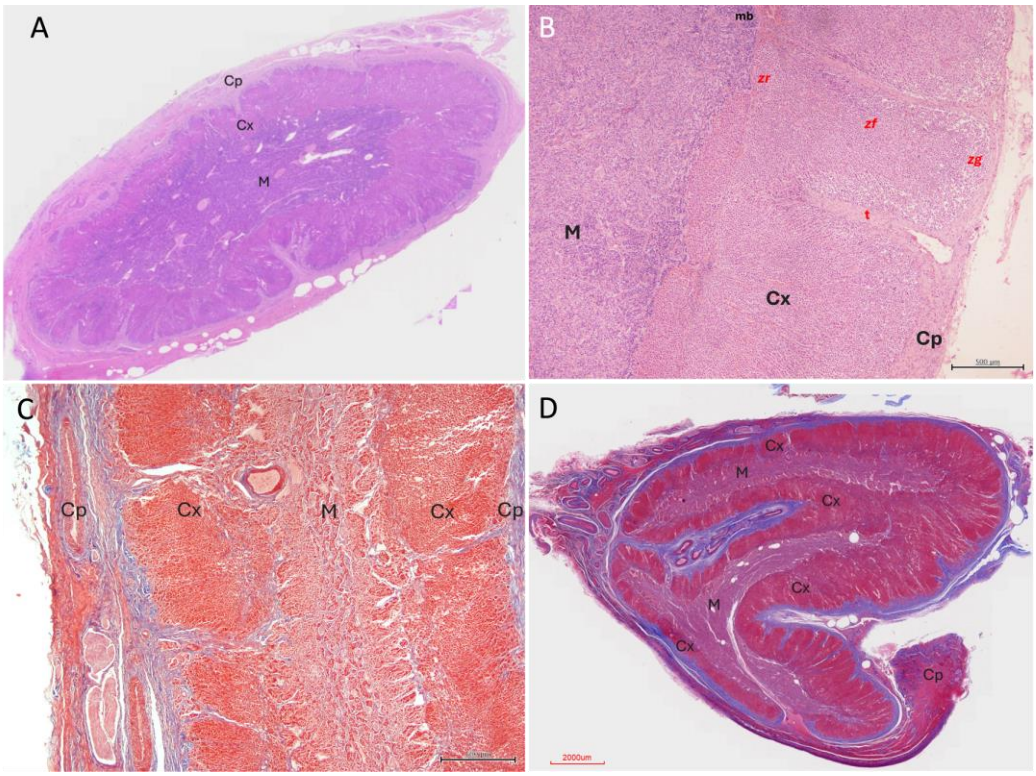

Figure 3. Architectural morphology of the adrenal gland in *Delphinus delphis*. (A) Submacroscopic view, Hematoxylin–Eosin (H-E), showing the overall adrenal architecture with clearly distinguishable capsule, cortex and medulla (M). (B) H-E section (4×) illustrating the capsule, cortex, and medulla (Cx = cortex; M = medulla; Cp = capsule). Connective tissue trabeculae (T) extend from the capsule into deeper regions of the gland. The three cortical zones are identifiable: zona glomerulosa (zg), zona fasciculata (zf), and zona reticularis (zr). (C) Masson's trichrome stain (MT) (4×) demonstrating the collagen-rich capsule and connective tissue trabeculae penetrating the cortex, creating a pseudolobular appearance. Vessels and nerve fibres are visible within the connective tissue. The cortex and medulla are clearly distinguishable. (D) MT stain, submacroscopic view showing a non-typical cortical–medullary arrangement. Rather than a simple peripheral cortex and central medulla, irregular distributions of cortical and medullary tissue are observed, with variable cortical compartmentalisation and two morphologically distinct medullary regions.

Although most glands exhibited the typical peripheral cortical and central medullary organisation, some specimens displayed a more complex architectural arrangement. In these cases, cortex and medulla were distributed in irregular, alternating layers rather than forming a simple concentric pattern (Figure 3D).

3.2.1. Capsule and Stromal Organisation

The adrenal gland was surrounded by a fibrous connective tissue capsule of variable thickness, which stained intensely with Masson's trichrome, highlighting its collagenous composition (Figures 3B, 4A, 4C). In some individuals, the capsule appeared thin and compact, whereas in others it was thicker and more irregular.

 doi:10.20944/preprints202603.1321.v1

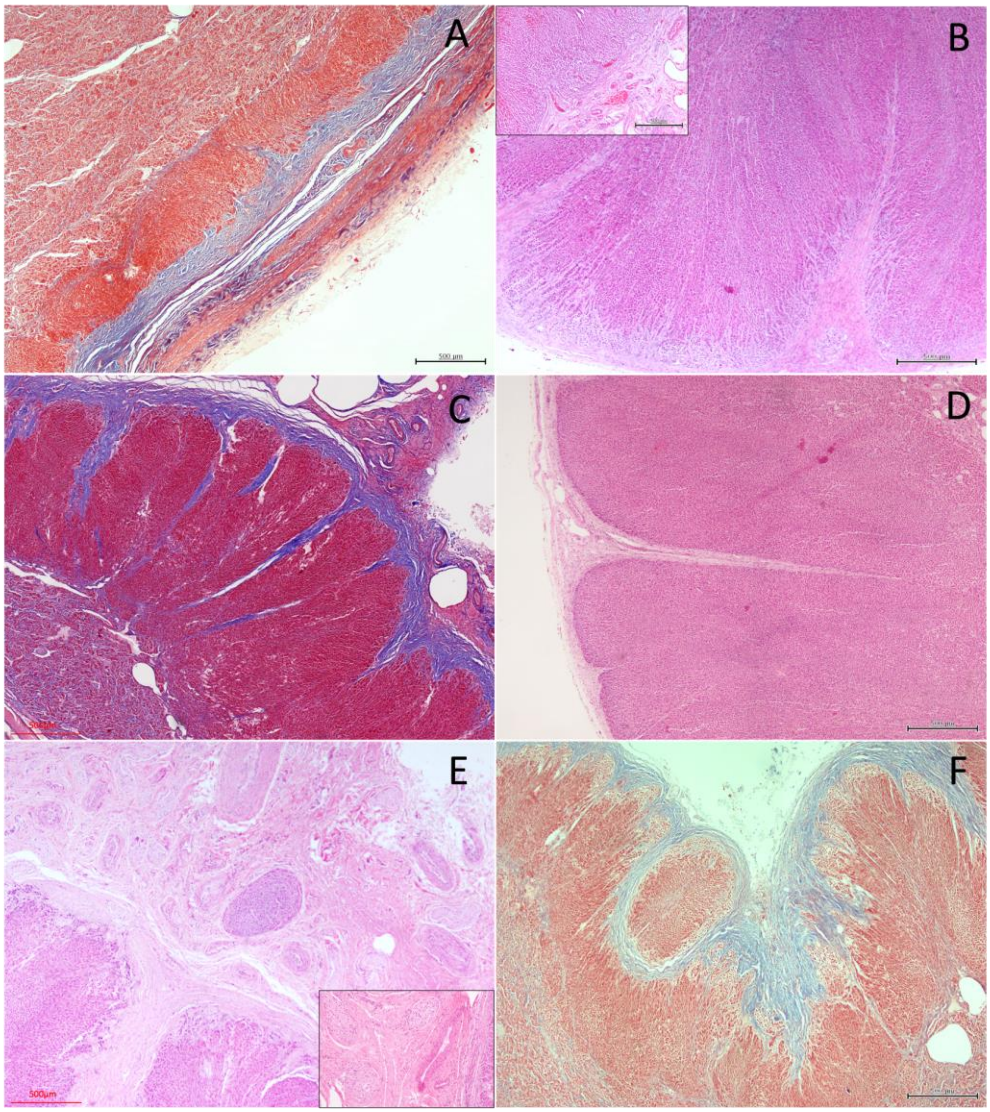

Figure 4. Capsular and stromal organisation of the adrenal gland in Delphinus delphis. (A) Masson's trichrome (MT) stain (4×) showing the fibrous capsule and underlying cortex. The capsule appears collagen-rich, and connective tissue trabeculae extend irregularly into the cortex. Thin connective septa are also visible at the cortico-medullary junction and, in places, extend delicately into the medulla; (B) Hematoxylin–Eosin (H-E, 4×) section illustrating trabecular projections of variable thickness penetrating the cortex. The inset (H-E, 4×) from the same adrenal highlights vascularisation within the capsular and subcapsular regions. (C) MT (2×) from a different individual demonstrating a more pronounced trabecular framework, producing a pseudolobular appearance of the cortex. Both shallow and deep trabeculae are observed, as well as thin connective septa extending into the medulla. (D) H-E (4×) section showing a relatively thin capsule with a slender but deeply penetrating trabecula extending into the zona fasciculata. (E) H-E (10×) detail of a thicker capsule containing numerous small- and medium-calibre blood vessels and associated nerve fibres. The inset (H-E, 10×) provides higher magnification of neural elements within the capsular connective tissue. (F) MT (4×) illustrating focal capsular invagination partially surrounding adjacent cortical tissue, forming an encapsulated cortical area that remains continuous with the surrounding cortex.

The capsule was moderately vascularised and contained small- to medium-calibre blood vessels frequently accompanied by nerve fibres within the pericapsular connective tissue (Figure 3A, 4B, 4E). These neurovascular structures extended inward along connective tissue trabeculae, forming a supporting stromal framework for the gland.

From the capsule, trabeculae projected irregularly into the cortex, forming a connective tissue network that supported and compartmentalised the adrenal parenchyma. These trabeculae were

 doi:10.20944/preprints202603.1321.v1

generally sparse and discontinuous, thinning as they progressed; however, in some specimens they penetrated deeply into the inner cortical zones, reaching the corticomedullary junction and occasionally extending into the medulla as thin septa (Figure 4). In such cases, trabecular extensions partially subdivided cortical tissue into compartment-like regions, contributing to variable internal architectural organisation.

Additionally, in some glands, small cortical regions adjacent to the capsule appeared partially or completely surrounded by capsular connective tissue. These areas remained morphologically continuous with the surrounding cortex and were interpreted as structural variations associated with capsular invagination or trabecular extension rather than discrete nodular formations. In these cases, cortical zonation appeared to reorganise concentrically around the connective tissue axis, with the three cortical layers (*zona glomerulosa*, *zona fasciculata*, and *zona reticularis*) re-established in sequence around the encapsulated region (Figure 4F).

3.2.2. Cortical Architecture

The adrenal cortex was organised into three distinct zones, identifiable on the basis of cellular arrangement and staining characteristics: the *zona glomerulosa*, *zona fasciculata*, and *zona reticularis*.

Cortical vascularisation was evident as a network of thin-walled sinusoidal capillaries distributed between the cell cords. These vessels were most clearly appreciable in the *zona fasciculata*, where they ran longitudinally between radially arranged cellular columns (Figure 4B). The sinusoids were lined by flattened endothelial cells and frequently contained erythrocytes. In the *zona glomerulosa*, smaller vascular profiles were observed interspersed among the rounded cellular clusters. Towards the cortico-medullary junction, vascular spaces appeared larger and more irregular in calibre (Figure 3B). Blood vessels were commonly associated with connective tissue septa and trabeculae extending inward from the capsule, forming a supportive stromal framework within the cortex. Masson's trichrome staining highlighted the collagenous components of these trabeculae and their close relationship with vascular structures (Figure 3C).

The outermost *zona glomerulosa* consisted of small, densely packed cells arranged in rounded or convex arched clusters beneath the capsule (Figure 5). These cells displayed relatively dark nuclei and scant cytoplasm in H-E staining. Periodic acid–Schiff–diastase (PAS-D) staining revealed limited cytoplasmic positivity in this zone. In contrast, Grimelius staining produced a marked argyrophilic reaction in the *zona glomerulosa*, with intense staining of the cellular clusters compared with the adjacent cortical layers (Figure 5E).

 doi:10.20944/preprints202603.1321.v1

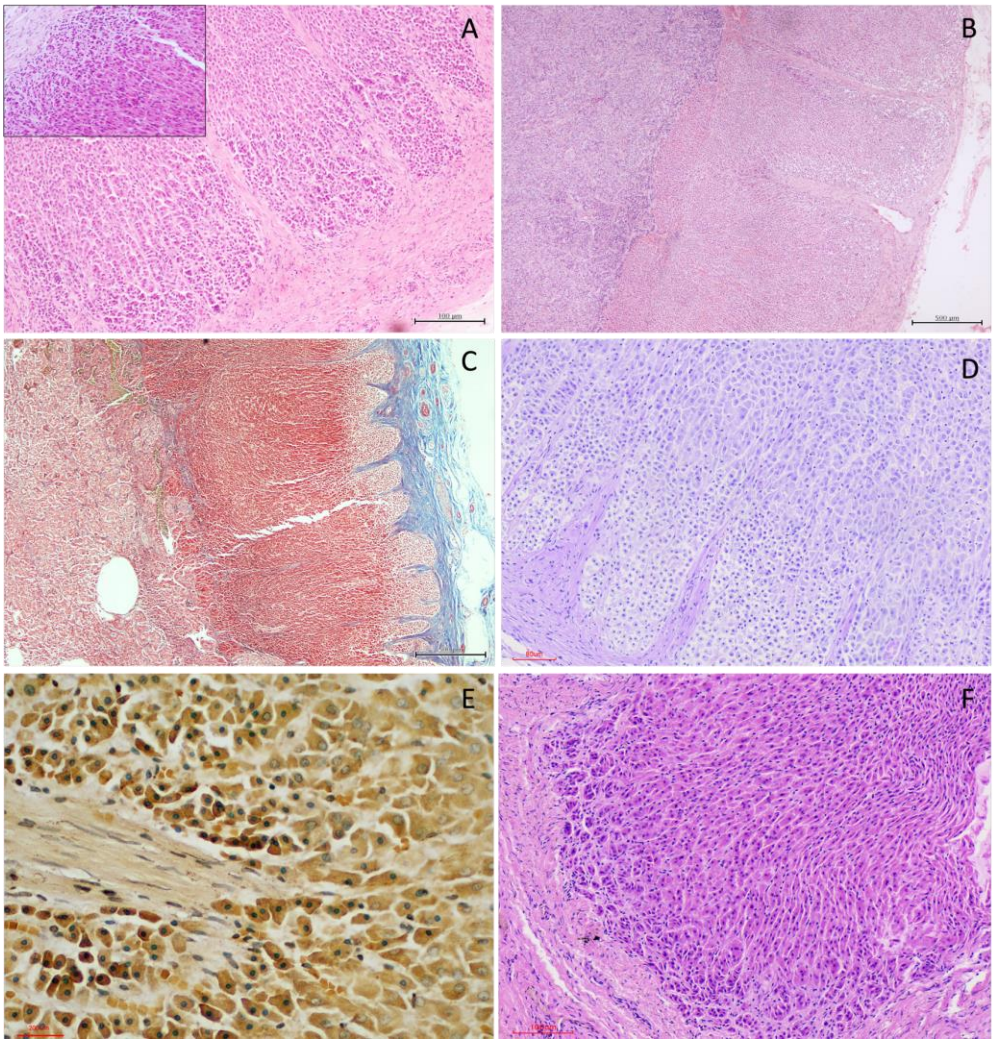

Figure 5. Histological characterisation of the zona glomerulosa in the adrenal cortex of *Delphinus delphis*. (A) Hematoxylin–Eosin (H-E, 10×) showing connective tissue trabeculae penetrating the cortex and a well-defined zona glomerulosa located immediately beneath the capsule. The inset (H-E, 4×) illustrates the overall cortical architecture and the arched arrangement of glomerular cell clusters along the capsular surface. (B) H-E (4×) section of the adrenal cortex demonstrating the three cortical zones. The zona glomerulosa forms a continuous subcapsular layer and extends along deep cortical trabeculae, appearing to re-establish its arched organisation wherever trabecular interfaces are present. Beneath it lies the zona fasciculata, composed of radially arranged cellular cords, followed by the zona reticularis adjacent to the medulla. (C) Masson's trichrome (MT) (4×) highlighting cortical zonation. The zona glomerulosa appears as a relatively thin, weakly stained subcapsular layer, sharply demarcated from the underlying zona fasciculata, which comprises the majority of the cortex. The zona reticularis is distinguishable adjacent to the medulla. A delicate connective tissue layer separates cortex and medulla. The medulla exhibits a dense vascular network and two chromaffin cell populations with differential staining intensity between peripheral and central regions. (D) Periodic acid–Schiff reaction with diastase stain (PAS-D) (10×) demonstrating zona glomerulosa cells beneath the capsule and their transition into the larger, more polygonal cells of the zona fasciculata. Glomerular cells appear smaller, with compact cytoplasm and darker nuclei compared with the more abundant, lightly stained cytoplasm of fasciculata cells. (E) Grimelius stain (20×) adjacent to a connective tissue trabecula. Zona glomerulosa cells show intense argyrophilic staining and relatively small cytoplasmic profiles, whereas adjacent zona fasciculata cells appear larger, polygonal, and comparatively less intensely stained. (F) H-E (10×) detail of the transition between zona glomerulosa and zona fasciculata, emphasising the change from rounded or arched glomerular clusters to straight fascicular cords of larger polygonal cells.

 doi:10.20944/preprints202603.1321.v1

The *zona fasciculata* formed the largest portion of the cortex and was composed of large polygonal cells arranged in straight or slightly curved cords oriented radially toward the medulla (Figure 6) . These cells exhibited abundant, lightly stained cytoplasm, and occasionally clear vacuoles on H-E sections, consistent with high lipid content, could be observed.

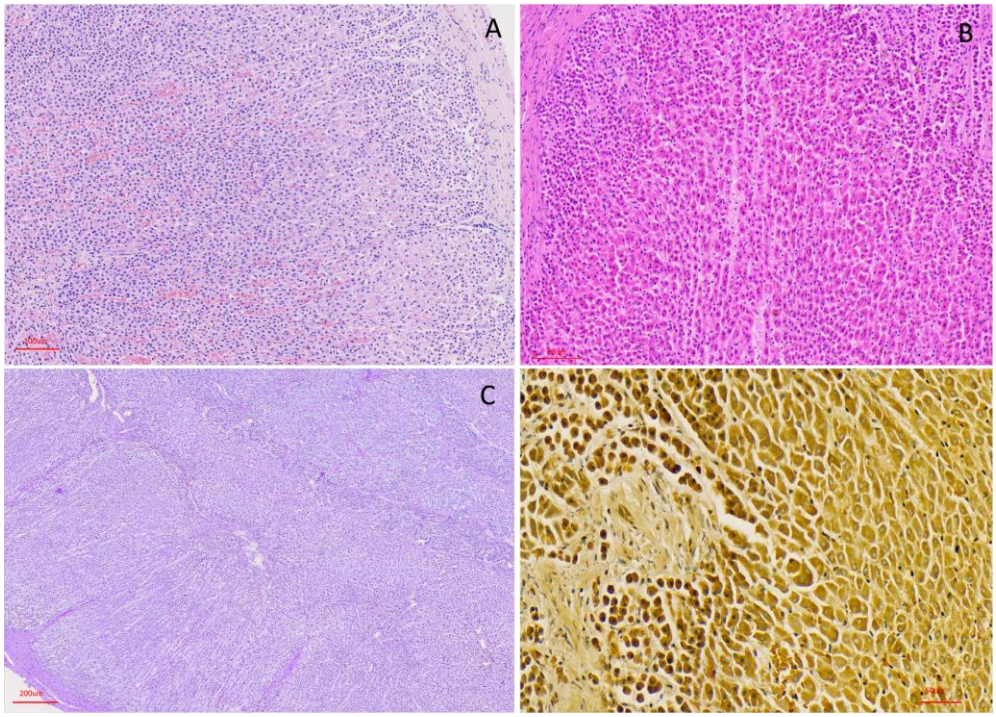

Figure 6. Histological organisation of the zona fasciculata and zona reticularis in the adrenal cortex of *Delphinus delphis*. (A) Hematoxylin–Eosin (H-E, 10×) section showing the zona fasciculata located beneath the zona glomerulosa and capsule. Fascicular cells are arranged in straight, parallel cords oriented radially toward the medulla. Sinusoidal vascular spaces are visible between the cellular cords. (B) H-E (20×) detail illustrating the polygonal morphology of zona fasciculata cells. These cells display abundant, lightly eosinophilic cytoplasm and centrally located nuclei. Sinusoids are interspersed between the cords, forming a regular vascular network. (C) Periodic acid–Schiff reaction with diastase stain (PAS-D) (4×) demonstrating the arrangement of fascicular cords beneath the zona glomerulosa. The zona fasciculata comprises the majority of the cortical thickness. A gradual transition toward the zona reticularis is observed adjacent to the medulla, where cells become smaller and more irregularly arranged. The zona reticularis exhibits a denser cellular network and borders the medullary region. (D) Grimelius stain (20×) highlighting differences between cortical zones. Zona fasciculata cells appear larger and polygonal with relatively lighter argyrophilic staining, whereas zona reticularis cells are smaller, more compact, and display stronger argyrophilic reactivity. Increased connective tissue and vascular elements are evident near the cortico-medullary junction.

The innermost *zona reticularis* consisted of smaller, more irregularly arranged cells forming an interconnected network of short cellular cords. Compared with the zona fasciculata, these cells displayed more eosinophilic cytoplasm and darker nuclei. In Grimelius stained sections, stronger argyrophilic was evident within this zone (Figure 6D), accentuating the distinction between these two inner cortical zones.

In one specimen, cortical tissue was observed surrounding medullary blood vessels, either as isolated cortical islands within the medulla or in association with deeply penetrating connective tissue trabeculae, resulting in focal intermingling of cortical and medullary elements. In this area, local reorganisation of cortical architecture was evident, with cortical layering re-established around the trabecular or vascular axis while maintaining the sequential arrangement of the three cortical zones (Figure 7A).

 doi:10.20944/preprints202603.1321.v1

In several specimens, marked vascular congestion was observed at the cortico-medullary junction. These changes were most evident in H-E stained sections and were localized primarily to the vascular transition zone between cortex and medulla. In some cases, focal erythrocyte extravasation within adjacent sinusoidal spaces was also observed (Figure 7B).

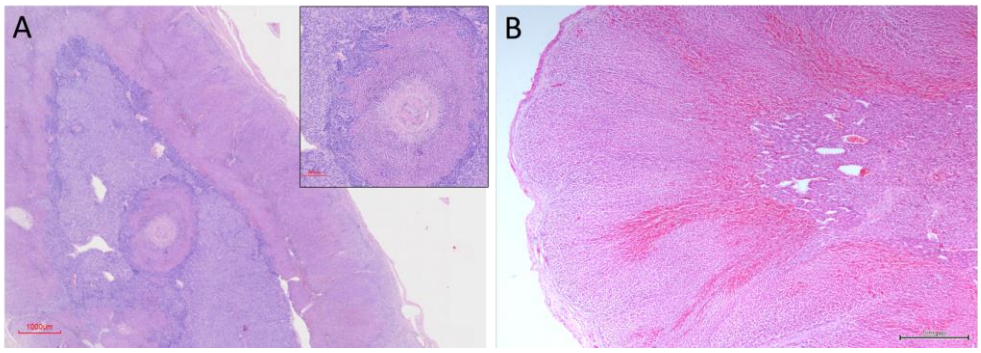

Figure 7. Cortical architectural reorganisation and corticomedullary vascularisation in the adrenal gland of Delphinus delphis. (A) Submacroscopic H-E section (3×) showing a large-calibre vessel within the medulla surrounded by concentrically organised cortical tissue. The inset (H-E, 10×) demonstrates the sequential arrangement of the three cortical layers re-established around the vascular structure; (B) H-E section (4×) illustrating marked vascular congestion at the cortico-medullary junction, characterised by dilation of vascular spaces.

3.2.3. Medullary Organisation

The adrenal medulla occupied the central region of the gland and was characterised by a dense vascular network, including numerous sinusoidal vessels and, in several specimens, one or more large-calibre venous channels consistent with a central medullary vein, that were not always located in a strictly central position (Figure 3A, 7A). These vessels were readily visible on H-E and MT staining and exhibited a more defined vascular wall compared with surrounding sinusoids.

Chromaffin cells were arranged in cords or clusters surrounding vascular spaces. Two chromaffin cell populations could be distinguished based on cytoplasmic appearance and staining intensity. A peripheral population of chromaffin cells forming a “medullary band” at the cortico-medullary interface, exhibited more basophilic cytoplasm, whereas more centrally located chromaffin cells appeared comparatively paler on H-E-stained sections (Figure 8).

 doi:10.20944/preprints202603.1321.v1

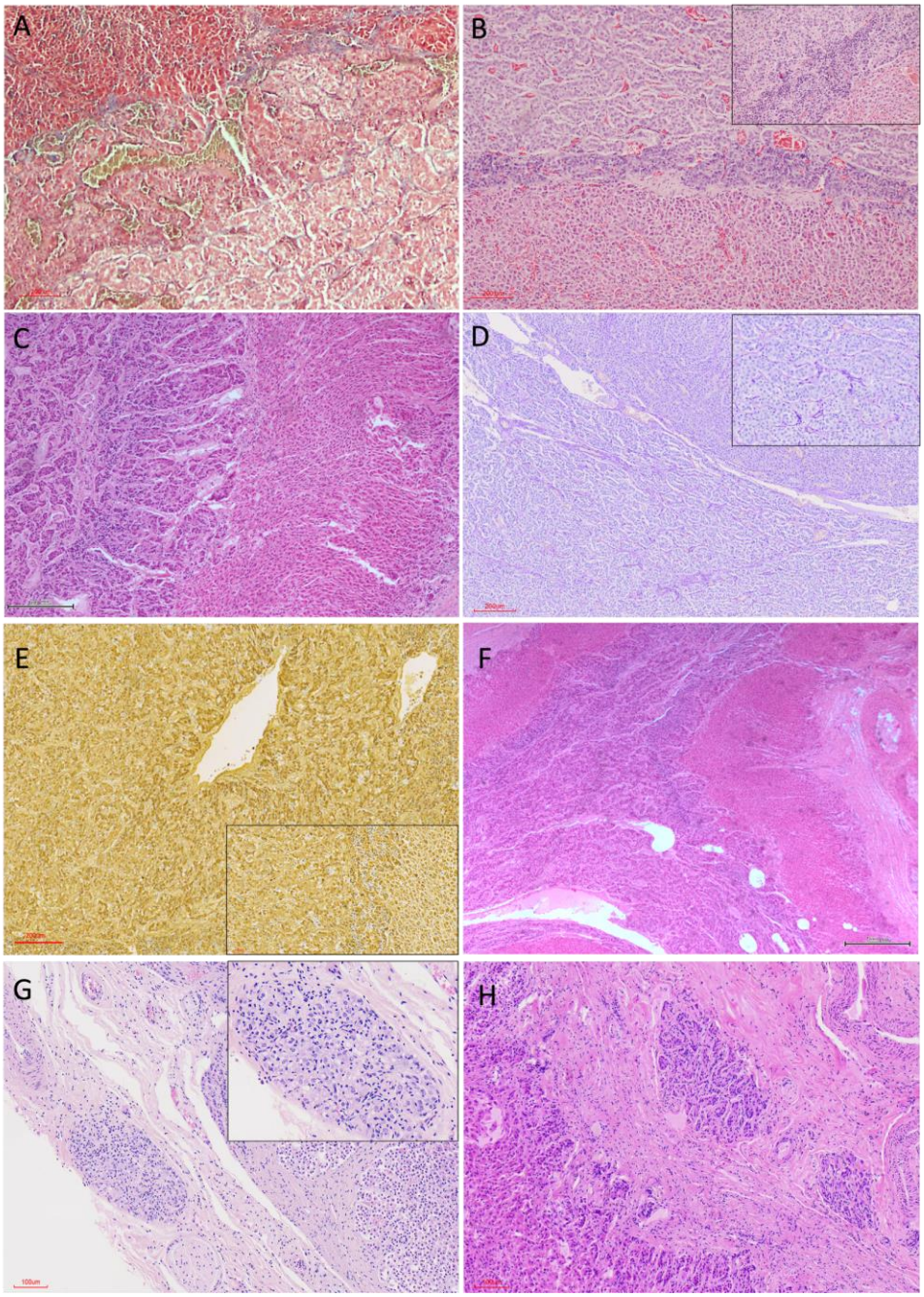

Figure 8. Medullary organisation and chromaffin cell distribution in the adrenal gland of *Delphinus delphis*. (A) Masson's trichrome (MT) stain (20×) demonstrating differential staining within the medulla. A peripheral chromaffin cell layer at the cortico-medullary junction forms a distinct "medullary band," distinguishable from more centrally located chromaffin cells. The dense vascular network of the medulla is evident. (B) Hematoxylin–Eosin (H-E, 10×) section of the cortico-medullary interface. The peripheral medullary band appears more basophilic compared with deeper medullary regions. Chromaffin cells are arranged in nests and rosette-like clusters among vascular spaces. The adjacent zona reticularis is identifiable within the cortex, separated from the medulla by a thin connective tissue interface. The inset illustrates regional variation in the thickness of the peripheral medullary band. (C) H-E (10×) section from a different individual showing a less sharply defined peripheral medullary band and increased interstitial connective tissue within the medulla, while maintaining differential staining between peripheral and central chromaffin populations. (D) Periodic acid-Schiff with diastase stain (PAS-D) (10×) of the cortico-medullary junction. The transition from zona fasciculata to zona reticularis is visible. The medulla displays nests of chromaffin cells arranged around a rich capillary bed. The inset highlights the rosette-like organisation of chromaffin cell clusters. (E) Grimelius stain (10×) of the medulla showing chromaffin cells arranged in compact clusters surrounding vascular spaces. Medium-calibre vessels are

 doi:10.20944/preprints202603.1321.v1

present within the medullary parenchyma. The inset (Grimelius, 10×) of the cortico-medullary junction demonstrates the clearly distinguishable peripheral and central chromaffin populations, with the cortex visible adjacent to the medulla. (F) H-E (10×) section illustrating the medulla with large- and medium-calibre vessels and connective septa extending within the medullary tissue. The peripheral medullary band and central chromaffin populations are distinguishable. Adjacent cortical tissue and capsule are visible, with prominent vascular structures. (G) H-E (10×; inset 20×) showing small aggregates of chromaffin-like cells within capsular connective tissue adjacent to vascular and neural elements. These focal cell clusters are morphologically similar to medullary chromaffin cells and remain continuous with adjacent adrenal parenchyma. (H) H-E (14×) demonstrating small chromaffin cell groups located within the capsule near the cortical boundary, exhibiting morphological characteristics consistent with medullary chromaffin populations.

Additionally, in a small number of cases, small aggregates of chromaffin-like cells were identified within the connective tissue of the capsule or along deep cortical trabeculae (Figure 8G, 8H). These cell clusters were sparse, focal, and morphologically similar to medullary chromaffin cells, appearing either adjacent to trabecular connective tissue or partially enclosed within capsular stroma, remaining structurally continuous with adjacent adrenal parenchyma.

3.3. Adrenal morphometry.

3.3.1. Adrenal Weight and Length in Sexually Mature Individuals

Absolute adrenal measurements in sexually mature *Delphinus delphis* showed overlapping distributions between sexes. Mean left adrenal weight was 7.44 ± 2.85 g in females (n = 12) and 7.22 ± 2.36 g in males (n = 12). Mean right adrenal weight was 7.17 ± 2.14 g in females and 6.99 ± 2.70 g in males.

Absolute adrenal length followed a similar pattern. Mean left adrenal length was 4.73 ± 0.77 cm in females (n = 18) and 4.99 ± 1.67 cm in males (n = 15), while mean right adrenal length was 4.77 ± 0.82 cm in females and 5.29 ± 1.05 cm in males.

Absolute adrenal morphometry by sex is provided in *Supplementary Figure S1.*

3.3.2. Body Size-Standardised Adrenal Morphometry Across Developmental Stages

The relationship between total body length and mean adrenal weight was assessed in individuals with complete body length data and adrenal weight measurement data (n = 41). Mean adrenal weight (calculated as the average of left and right glands when both were available) showed a positive association with body *length (Spearman's* $\rho = 0.77$, $p = 4.51 \times 10^{-9}$*; Figure 9).*

 doi:10.20944/preprints202603.1321.v1

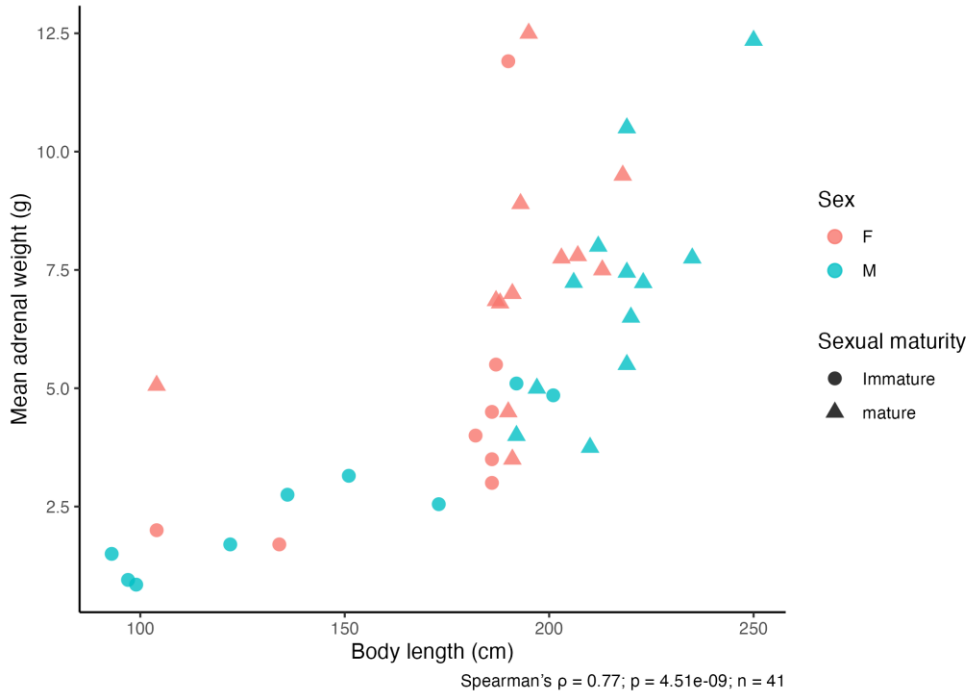

Figure 9. Relationship between body length and adrenal weight in *Delphinus delphis***.** Scatterplot showing the association between total body length and mean adrenal weight (calculated as the average of left and right adrenal glands) across all individuals. The relationship was assessed using Spearman's rank correlation ($\varrho = 0.77$, $p = 4.51 \times 10^{-9}$).

When expressed relative to body length, adrenal weight and length were calculated for all individuals with available measurements. Sample sizes differed slightly between left and right glands due to incomplete data (Figure 10).

Body size–standardised adrenal morphometry in Delphinus delphis

Adrenal weight and length expressed relative to body length

n (Left)	n (Right)	Adrenal weight – Left (g/cm) — mean ± SD	Adrenal weight – Right (g/cm) — mean ± SD	Adrenal length – Left (cm/cm) — mean ± SD	Adrenal length – Right (cm/cm) — mean ± SD
41	40	0.0295 ± 0.0141	0.0299 ± 0.0133	0.0236 ± 0.0067	0.0248 ± 0.0062

Values are expressed as mean ± standard deviation.

Figure 10. Body size–standardised adrenal morphometry in *Delphinus delphis*. Adrenal weight (g/cm) and length (cm/cm) expressed relative to total body length across all individuals included in the study. Values are presented as mean ± standard deviation. Adrenal measurements were standardised by body length to account for inter-individual differences in body size. Sample sizes (n) are reported separately for left and right glands due to incomplete measurements in some individuals. Adrenal measurements were standardised by body length to account for inter-individual differences in body size.

3.3.3. Corticomedullary Ratio (CM)

The histological corticomedullary ratio (CM) was calculated separately for left and right adrenal glands as the sum of cortical thickness measured on both sides of the medulla divided by medullary thickness. CM values were obtained for 50 left and 48 right adrenal glands (Figure 11).

Paired comparison between left and right glands revealed no significant difference (Wilcoxon signed-rank test: $V = 294.5$, $p = 0.12$), indicating the absence of lateral asymmetry.

 doi:10.20944/preprints202603.1321.v1

Corticomedullary ratio (CM)					
n (Left)	Median (Left)	IQR (Left)	n (Right)	Median (Right)	IQR (Right)
50.00	0.94	0.81	48.00	1.00	0.83

Figure 11. Left and right corticomedullary ratio (CM) descriptive statistics in Delphinus delphis. Descriptive statistics of the histological corticomedullary ratio (CM) presented separately for left and right adrenal glands. Values are expressed as median and interquartile range (IQR). Sample sizes (n) are reported independently for each side due to incomplete measurements in some individuals. These data support the assessment of lateral symmetry prior to side-averaged analyses.

In the absence of significant side-related differences, CM values were averaged per individual (mean of left and right glands when available), generating a single per-individual CM value for subsequent analyses.

When analysed according to sexual maturity, CM differed significantly between sexually immature (n = 16) and mature (n = 34) individuals (Wilcoxon rank-sum test: W = 113.5, p = 0.0010). Mature individuals exhibited higher median CM values (1.04, IQR 0.85) compared to immature individuals (0.60, IQR 0.34) (Figure S2, Figure 12).

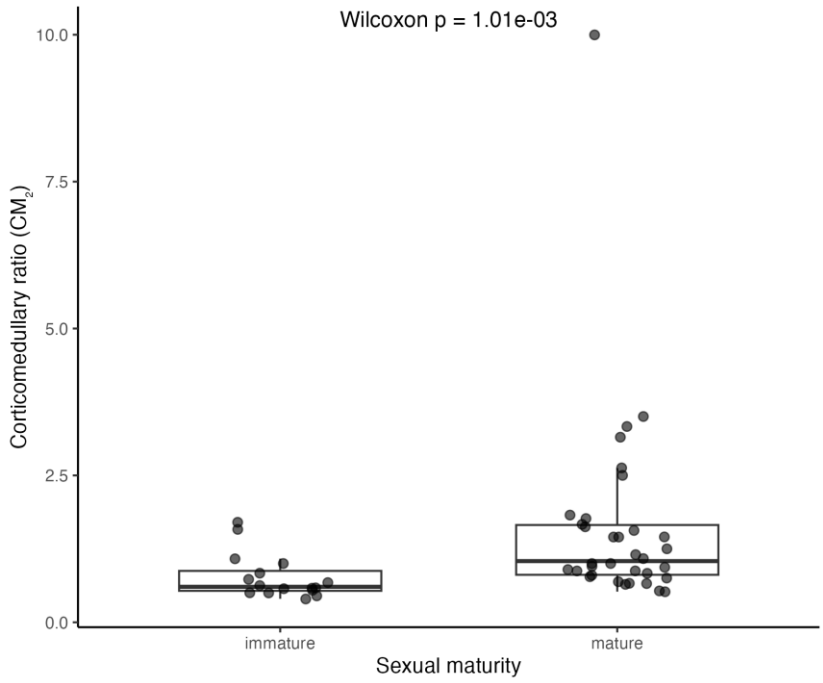

Figure 12. Corticomedullary ratio (CM) in relation to sexual maturity in *Delphinus delphis*. Boxplots showing per-individual CM values (mean of left and right adrenal glands when available) in sexually immature (n = 16) and mature (n = 34) individuals. Boxes represent the median and interquartile range (IQR), with individual data points overlaid. A significant difference was detected between groups (Wilcoxon rank-sum test: W = 113.5, p = 0.0010), with mature individuals exhibiting higher CM values overall.

In sexually mature individuals, CM values were further evaluated in relation to cause of death (COD). Animals were classified as Acute COD (fishing interaction; n = 10) or Non-acute COD (infectious, parasitic, or medical/degenerative causes; n = 18). Median CM_2 was 1.02 (IQR 2.25) in the Acute COD group and 1.27 (IQR 0.77) in the Non-acute COD group. The Acute COD group showed greater variability, largely influenced by one individual exhibiting an unusually high CM value. Despite a numerically higher median in the Non-acute COD group, no statistically significant difference was detected between groups (Wilcoxon rank-sum test: W = 95, p = 0.8291) (Figure S3, Figure 13).

 doi:10.20944/preprints202603.1321.v1

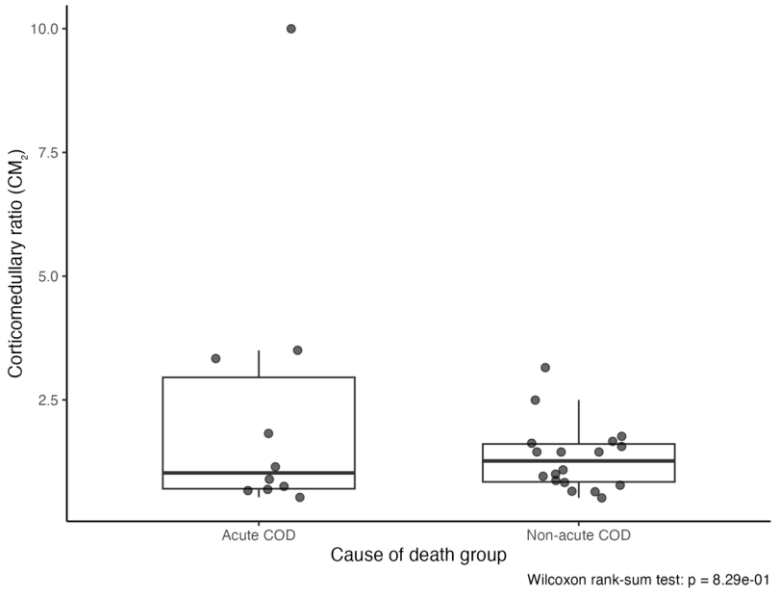

Figure 13. Corticomedullary ratio (CM) in adult *Delphinus delphis* according to cause of death Per-individual CM values (mean of left and right adrenal glands) in sexually mature animals classified as Acute COD (fishing interaction; n = 10) and Non-acute COD (infectious, parasitic, or medical/degenerative causes; n = 18). Boxes represent the median and IQR, with individual data points shown. No significant difference was detected between groups (Wilcoxon rank-sum test: W = 95, p = 0.8291).

3.4 Ultrastructural Study

Transmission electron microscopy (TEM) revealed a well-organized adrenal gland displaying a clear cortical–medullary differentiation. Distinct ultrastructural features were observed in each cortical zone as well as in the adrenal medulla, where two populations of chromaffin cells were identified based on the morphology of their secretory granules. A rich vascular network composed of fenestrated capillaries within the cortex and sinusoidal vessels within the medulla were observed. Endocrine cells were closely apposed to vascular endothelium. Amyelinated nerve fibers were observed in the interstitial spaces of the adrenal gland, in close association with both cortical and medullary cells (Figure 14).

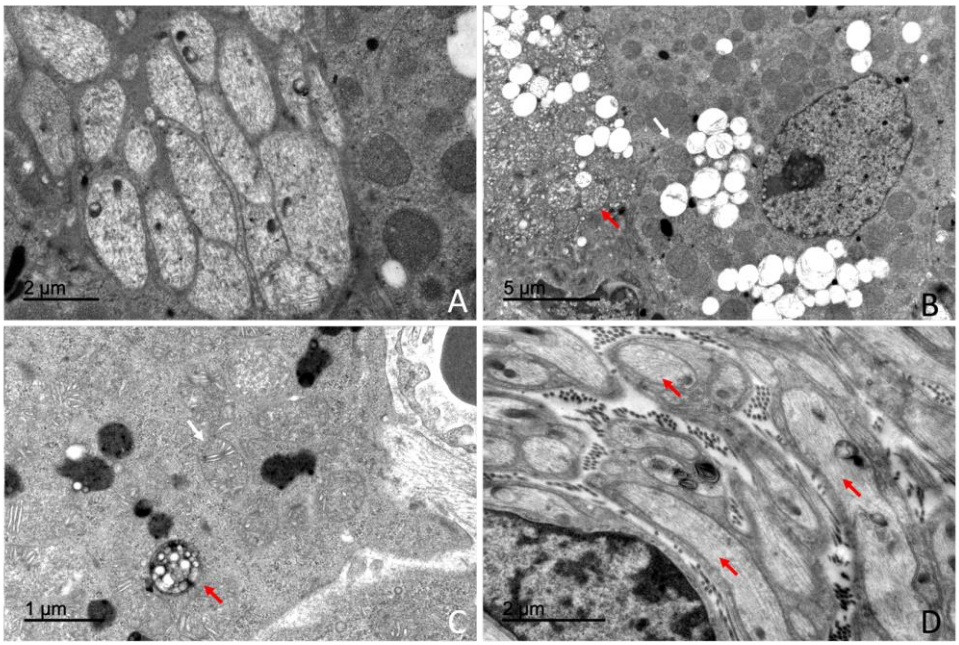

 doi:10.20944/preprints202603.1321.v1

Figure 14. Transmission electron microscopy illustrating general ultrastructural features of the adrenal gland and associated innervation. (A) Amyelinated nerve fibers located within the interstitial space. (B) Cortical spongiocyte showing cytoplasmic degeneration (red arrow) adjacent to a morphologically normal cell (white arrow). (C) Zona reticularis cell displaying an autophagosome (red arrow), digitiform mitochondria (white arrow), and electron-dense lysosomes. (D) Amyelinated nerve fibers observed in close association with adrenal parenchymal cells (red arrows).

3.4.1 Adrenal Cortex

Transmission electron microscopy revealed that the adrenal cortex was organized into three distinct cellular zones: *the zona glomerulosa, zona fasciculata, and zona reticularis*. Each cortical zone was composed of cells with characteristic ultrastructural features, including differences in cytoplasmic organization, organelle abundance, and the presence of lipid droplets.

Ultrastructural morphometric measurements were performed to quantify mean cell diameter in each cortical zone and in medullary chromaffin cell types. Mean cell diameter (μm) values are summarised in Table 1.

Table 1. Mean cell diameter (μm) of adrenal cortical and medullary cells in Delphinus delphis.

Cell type	Juveniles	Adult female	Adult males
Zona glomerulosa	16.34 ± 0.46	16.61 ± 0.98	16.48 ± 0.62
Zona fasciculata	16.66 ± 0.79	16.75 ± 0.51	16.81 ± 0.78
Zona reticularis	16.06 ± 0.36	16.20 ± 0.62	16.16 ± 0.51

Values are expressed as mean ± standard deviation (SD). Juvenile values represent pooled measurements from two individuals (n = 2), whereas adult female and adult male values correspond to single individuals (n = 1 each) and reflect intra-individual variability.

3.4.1.1. Zona Glomerulosa

Cells of the *zona glomerulosa* were arranged in compact clusters or glomeruli. Cells displayed a polygonal morphology and contained centrally located, round to oval nuclei with predominantly euchromatic chromatin and small heterochromatin aggregates (Figure 15).

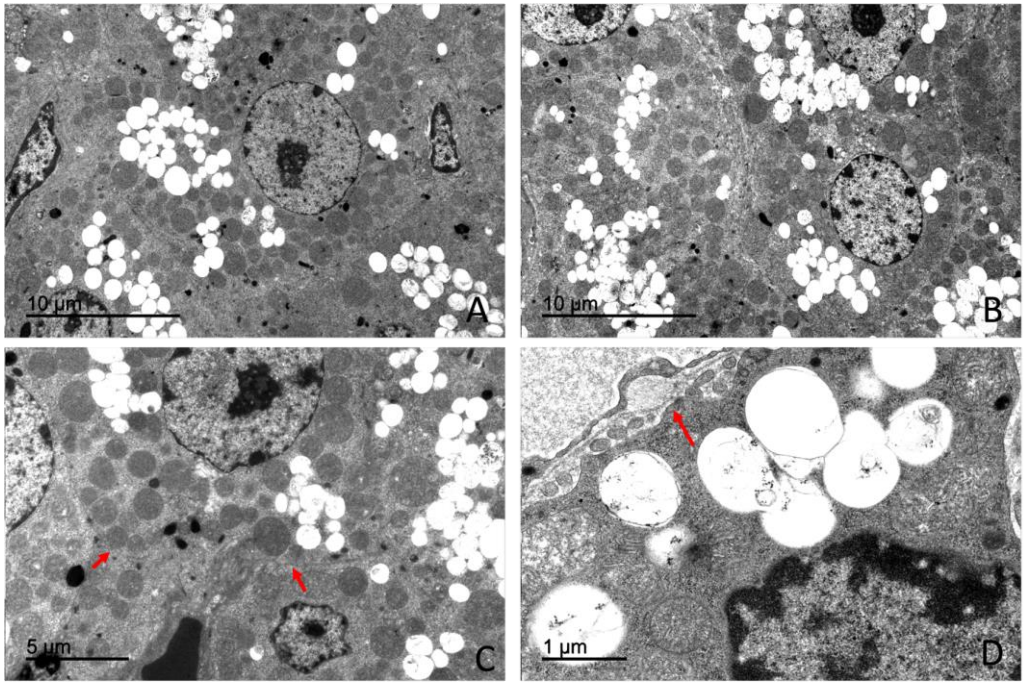

 doi:10.20944/preprints202603.1321.v1

Figure 15. Transmission electron microscopy of the zona glomerulosa of the adrenal cortex in Delphinus delphis. (A) Glomerulosa cells arranged in compact, mosaic-like clusters. (B) Detail of glomerulosa cells showing digitiform mitochondria and lipid droplets. (C) Additional view of the mosaic organization characteristic of the zona glomerulosa (red arrows). (D) Glomerulosa cell in close association with a fenestrated capillary (red arrow).

The cytoplasm was characterized by abundant smooth endoplasmic reticulum, numerous lipid droplets, and a high density of mitochondria with tubular or digitiform cristae lacking elementary particles. Mitochondria exhibited a mean diameter ranging between 545 and 555 nm across age and sex categories. Lipid droplets displayed a mean diameter of approximately 645-660 nm, depending on the animal soubgroup, and were observed either isolated or forming small clusters within the cytoplasm (Table S3).

3.4.1.2. Zona Fasciculata

Cells of the zona fasciculata were large and arranged in cords. These cells exhibited a markedly electron-lucent cytoplasm (Figure 16).

Numerous lipid droplets occupied extensive areas of the cytoplasm. These lipid droplets were membrane-bound, showed an electron-lucent content and displayed a mean diameter of approximately **660–680 nm**, depending on the animal subgroup. The cytoplasm was characterized by the presence of an extensive smooth endoplasmic reticulum occupying large cytoplasmic regions. Numerous mitochondria with digitiform cristae lacking elementary particles showing an average diameter of approximately **575–580 nm** were also observed (Table S3)

Rough endoplasmic reticulum and Golgi complexes were present, whereas lysosomes were scarce. Nuclei were generally round to oval and predominantly euchromatic.

Occasional fasciculata cells exhibited ultrastructural features consistent with cytoplasmic degeneration, including vacuolization and organelle disorganization (Figure 14B).

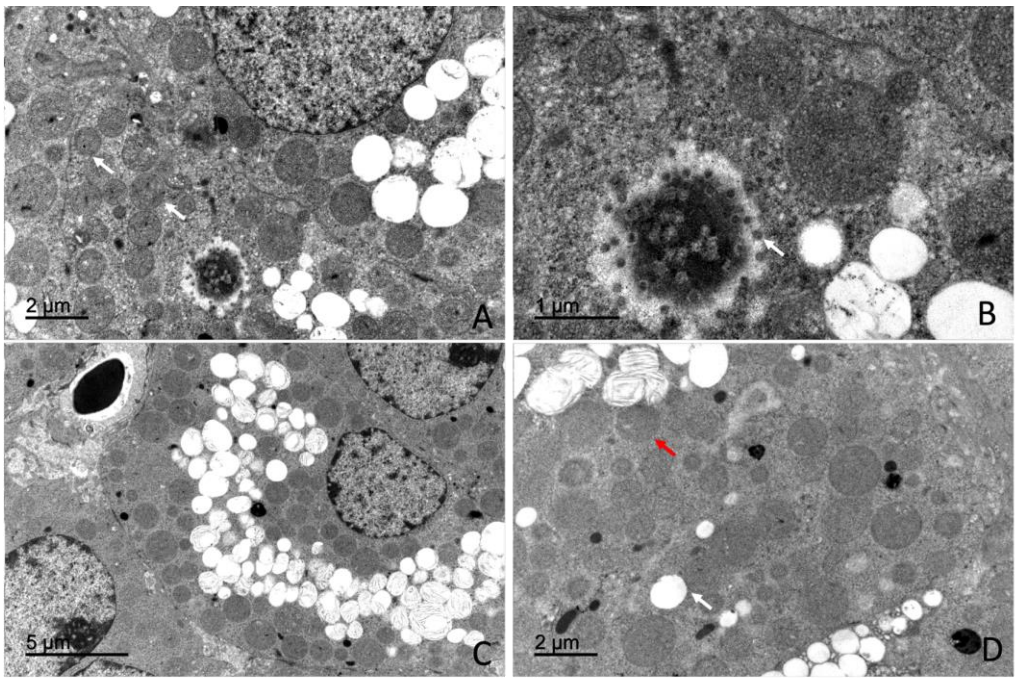

Figure 16. Transmission electron microscopy showing characteristic features of the zona fasciculata in Delphinus delphis. (A) Fasciculata cell with abundant mitochondria distributed throughout the cytoplasm (white arrows); (B) Nucleus of a fasciculata cell exhibiting prominent nuclear pores (white arrow); (C) Spongiocyte with numerous lipid droplets occupying most of the cytoplasm; (D) Spongiocyte displaying abundant mitochondria (red arrow) and lipid droplets of varying size (white arrows).

3.4.1.3. Zona Reticularis

 doi:10.20944/preprints202603.1321.v1

Cells of the zona reticularis were smaller and more compactly arranged than those of the zona fasciculata. The cytoplasm exhibited increased electron density (Figure 17).

Compared with glomerulosa and fasciculata cells, zona reticularis cells showed a reduced abundance of smooth endoplasmic reticulum, lipid droplets, and mitochondria, although mitochondria displayed a pleomorphic morphology. Rough endoplasmic reticulum and Golgi complexes were present. The presence of autophagosomes was observed occasionally (Figure 14C).

A high number of pleomorphic lysosomes was observed and represented a distinctive morphological feature of these cells (Figure 17). Electron-dense inclusions of variable size and morphology, consistent with residual bodies or lipofuscin-like material, were frequently observed in the cytoplasm. Nuclei showed irregular contours and an increased proportion of heterochromatin.

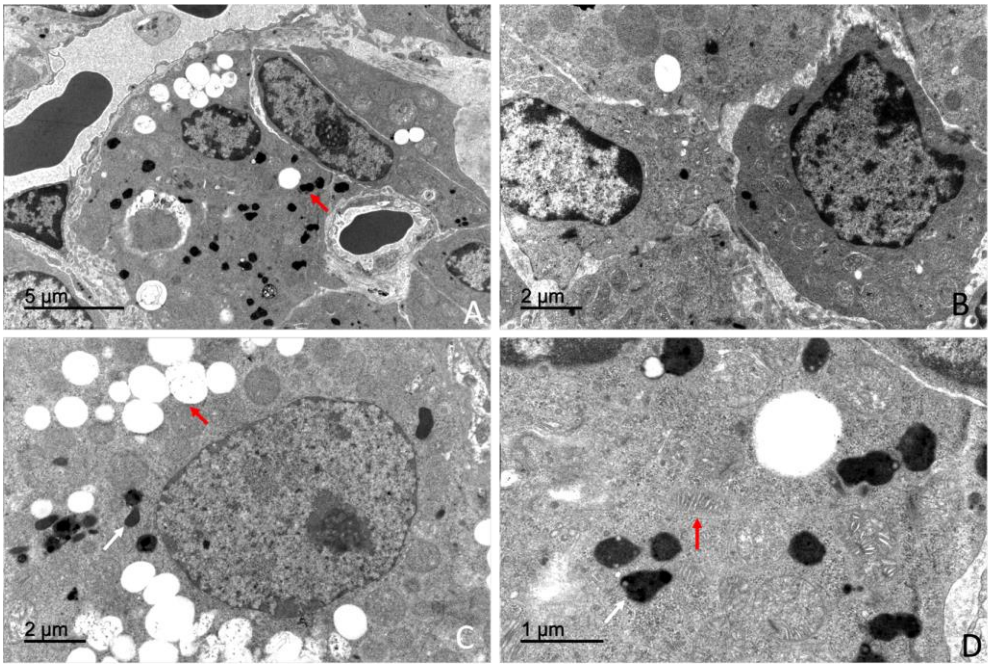

Figure 17. Transmission electron microscopy of zona reticularis cells in Delphinus delphis. (A) Reticular cells characterized by abundant electron-dense lysosomes (red arrow); (B) Irregular arrangement of zona reticularis cells within the cortex; (C) Cytoplasm of a reticular cell containing clusters of lipid droplets (red arrow) and lysosomes (white arrow); (D) Reticular cell showing digitiform mitochondria (red arrow) and dense lysosomes (white arrow).

Morphometric analysis showed that lipid droplets in zona reticularis cells exhibited mean diameters of approximately **650–670 nm,** while mitochondria presented mean diameters of approximately **574–584 nm (Table S3).**

A comparative overview of mitochondrial and lipid droplet diameters across cortical zones is presented in Figure 18.

 doi:10.20944/preprints202603.1321.v1

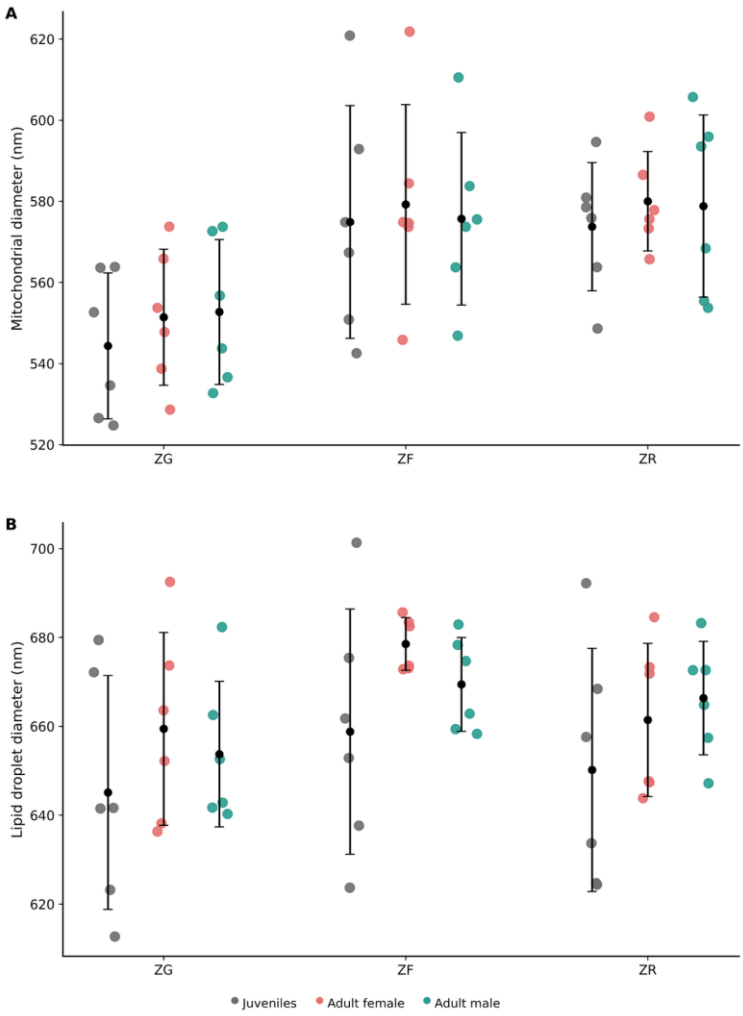

Figure 18. Ultrastructural morphometric analysis of adrenal cortical organelles in Delphinus delphis. (A) Mean mitochondrial diameter (nm) in zona glomerulosa (ZG), zona fasciculata (ZF), and zona reticularis (ZR) cells.(B) Mean lipid droplet diameter (nm) in the same cortical zones. Each dot represents an individual measurement (n = 6 per group). Black symbols indicate mean ± SD. Juvenile values represent pooled measurements from two individuals (n = 2), whereas adult female and adult male values correspond to single individuals (n = 1 each) and reflect intra-individual variability.

3.4.2. Adrenal Medulla

Transmission electron microscopy revealed that the adrenal medulla was composed predominantly of chromaffin cells arranged in close association with vascular structures. Two chromaffin cell populations were identified based on their ultrastructural characteristics, particularly the morphology and electron density of their secretory granules.

Morphometric analyses were performed to quantify granule size and mean cell diameter across animal subgroups. Mean cell diameter values for medullary chromaffin cells are presented in Table S4.

3.4.2.1. Chromaffin Cells Type A

Type adrenaline (A) chromaffin cells were characterized by a cytoplasm densely filled with numerous membrane-bound secretory granules (Figure 19A,19B). These cells were organised in a palisade arrangement below the cortical area.

 doi:10.20944/preprints202603.1321.v1

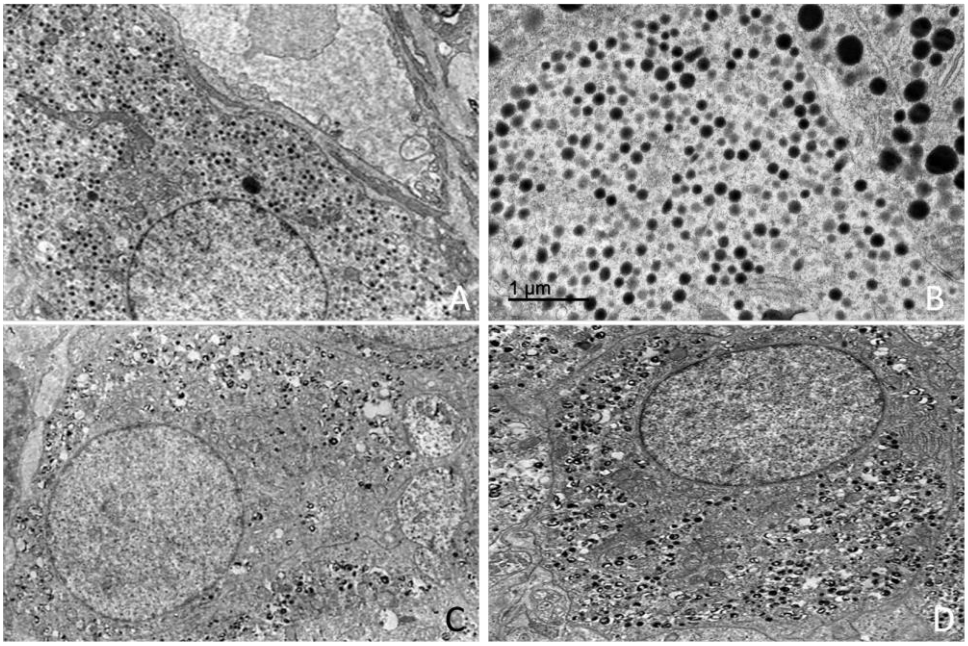

Figure 19. Transmission electron microscopy of chromaffin cells in the adrenal medulla. (A, B) Chromaffin cells type A characterized by numerous small, homogeneous, electron-dense secretory granules; (C, D) Chromaffin cells type NA showing pleomorphic secretory granules with heterogeneous electron density and a prominent electron-lucent halo.

The secretory granules were predominantly electron-dense, relatively homogeneous in size, and exhibited a narrow or poorly defined electron-lucent halo. Granules were diffusely distributed throughout the cytoplasm. Morphometric analysis revealed a *Granule diameter measured 375.05 ± 29.83 nm in juveniles, 383.52 ± 24.85 nm in the adult female, and 385.56 ± 17.62 nm in the adult male* (Table S4).

The cytoplasm also contained rough endoplasmic reticulum and Golgi complexes. Mitochondria were present and did not display distinctive ultrastructural features. Nuclei were generally large and predominantly euchromatic, with finely dispersed chromatin.

3.4.2.2. Chromaffin Cells Type NA

Type noradrenaline (NA) chromaffin cells had a scattered distribuition and exhibited a cytoplasm densely packed with membrane-bound secretory granules showing marked heterogeneity in size and electron density (Figure 19C,19D).

Secretory granule diameter was slightly smaller in type NA cells compared to type A cells across all animal subgroups. These were characterized by an eccentrically located electron-dense core surrounded by a wide and well-defined electron-lucent halo. Granules were abundantly distributed throughout the cytoplasm and occasionally formed clusters. Granule diameter measured 364.14 ± 32.65 nm in juveniles, 362.50 ± 27.14 nm in the adult female, and 363.71 ± 31.59 nm in the adult male (Table S4).

The cytoplasm contained rough endoplasmic reticulum and Golgi complexes, mainly in perinuclear regions. Mitochondria were present without distinctive ultrastructural features. Nuclei were large, round to oval, and predominantly euchromatic.

Mean chromaffin cell diameter values were comparable across age and sex categories in both cell types. Granule diameter was consistently higher in type A cells than in type NA cells across all subgroups. A comparative morphometric overview is presented in Figure 20.

 doi:10.20944/preprints202603.1321.v1

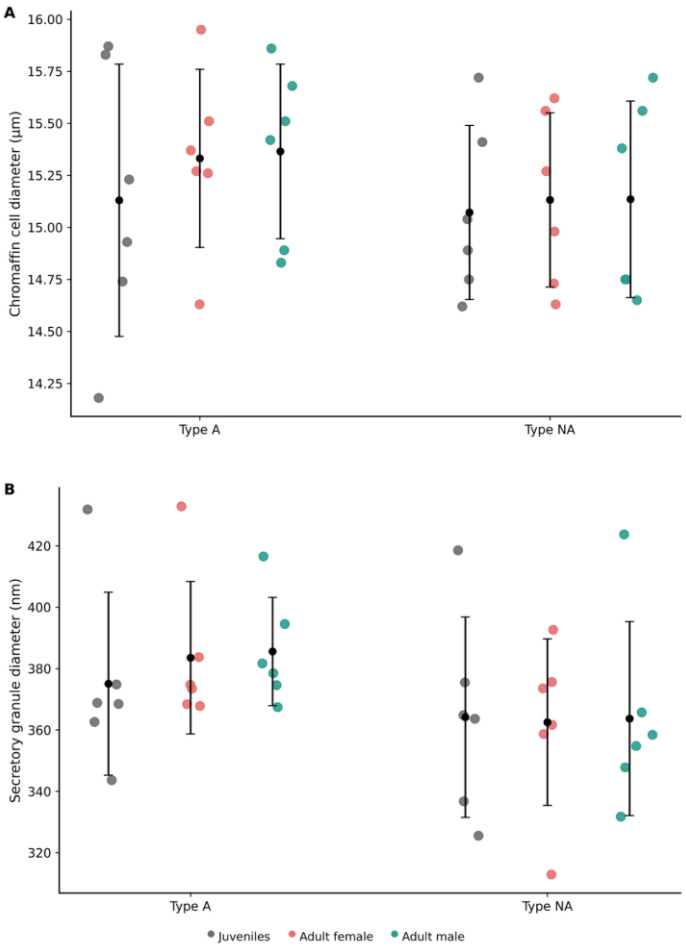

Figure 20. Ultrastructural morphometric analysis of adrenal medullary chromaffin cells in *Delphinus delphis*. (A) Mean chromaffin cell diameter (µm) in type A (adrenaline) and type NA (noradrenaline) chromaffin cells. (B) Mean secretory granule diameter (nm) in type A and type NA chromaffin cells. Each dot represents an individual measurement (n = 6 per group). Black symbols indicate mean ± SD. Juvenile values represent pooled measurements from two individuals (n = 2), whereas adult female and adult male values correspond to single individuals (n = 1 each) and reflect intra-individual variability.

4. Discussion

This study integrates gross, histological, morphometric, and ultrastructural analyses to examine adrenal gland organization in the short beaked common dolphin (Delphinus delphis). The combined approach enables intra-specific evaluation and comparative interpretation across delphinids.

4.1 Gross and Histological Architecture of the Gland

The adrenal glands of Delphinus delphis conformed to the general odontocete pattern. Cross-sections were predominantly oval, and left and right glands were broadly symmetrical, with only minor inter-individual variation. This contrasts with the more polygonal outline described in the common bottlenose dolphin (*Tursiops truncatus*) *[27]*. Connective tissue septation followed the typical delphinid arrangement: capsular trabeculae extended toward the cortico-medullary boundary and occasionally continued as fine septa into the medulla, similar to descriptions in other dolphin species *[26–28,30,38,39]*. This pattern supports their interpretation as architectural variants rather than structural abnormalities.

In one gland, a medium-caliber artery penetrated deeply into the parenchyma, accompanied by a sleeve of cortical tissue maintaining recognizable zonal organization along its course toward the

 doi:10.20944/preprints202603.1321.v1

medulla. Similar configurations have been described in ungulates and in the common bottlenose dolphin, where penetrating vessels ensheathed by cortical layers extend into the medulla [27,40]. Such vascular-associated cortical invaginations are generally interpreted as growth-related architectural variants [26]. Although somatic growth stabilizes after sexual maturity in cetaceans, endocrine organs may continue to increase in mass at a slower rate [26,41]. The presence of this configuration in a large, sexually mature individual therefore supports a developmental rather than pathological interpretation.

From a developmental perspective, the adrenal gland reflects the distinct embryological origins of cortex and medulla [42]. Irregular cortical projections, intramedullary cortical nodules, and vascular-associated cortical inclusions have been documented in humans, rodents, and domestic ungulates and are typically regarded as non-pathological variants related to developmental patterns or postnatal structural development [43–45].

Occasional clusters of chromaffin-like cells were identified within the capsule and along cortical trabeculae. Comparable capsular aggregates have been described in the bottlenose dolphin and interpreted as accessory adrenal tissue [27,28]. In terrestrial mammals, extra-medullary chromaffin tissue has been reported along vascular routes and within connective septa, often linked to developmental migration [46–48]. Given the close cortico–medullary interaction within the adrenal gland, where cortical glucocorticoids influence catecholamine synthesis through paracrine mechanisms [49,50], the proximity of chromaffin cells to cortical tissue and penetrating vessels in Delphinus delphis likely reflects functional integration rather than architectural irregularity.

Cortical zonation followed the classical three-layered organization. In contrast to the findings in common bottlenose dolphins, where a thin zona intermedia was described beneath the zona glomerulosa, no distinct intermediate layer was identified here. Transitional cortical layers have been reported inconsistently in other mammals, including humans [51–54], and their absence in *Delphinus delphis* supports interspecific variability in cortical microarchitecture across dolphin species. A peripheral band of intensely basophilic chromaffin cells was consistently observed at the cortico-medullary interface, corresponding to the “medullary band” described in common bottlenose dolphins, pantropical spotted dolphin (*Stenella attenuata*) and in the spinner dolphin (*Stenella longirostris*) *[26–28]*, indicating that this arrangement represents a conserved mammalian pattern rather than a cetacean-specific specialization [55–57].

In several individuals, vascular congestion was observed at the cortico-medullary junction, occasionally accompanied by focal erythrocyte extravasation. These changes were not associated with disruption of adrenal architecture and were localized primarily to the vascular transition zone between cortex and medulla. The adrenal gland exhibits a centripetal vascular organization in which cortical sinusoidal blood flows toward the medulla before draining through the central vein, creating a vascular convergence zone at the cortico-medullary interface [58,59]. During acute physiological stress, simultaneous activation of the HPA axis and the sympathoadrenal system is accompanied by increased adrenal perfusion and intense catecholamine release, processes that may promote sinusoidal dilation and vascular congestion [60,61]. Comparable adrenal vascular alterations have been described in other wildlife species exposed to extreme physiological stress, including capture or stranding events, where they are interpreted as part of the systemic stress response [62]. Further pathological investigations integrating endocrine, vascular, and histopathological parameters would be required to clarify the biological significance of these findings in stranded cetaceans.

The present dataset comprised a substantial intra-specific sample collected over an extended period and including individuals that died under both acute and chronic conditions. This allowed evaluation of adrenal architecture across diverse physiological and pathological contexts within a single species. Previous studies suggested that architectural irregularities may be more frequent in stranded *T. truncatus* than in exclusively bycaught *Stenella* species *[27,28]*; however, those comparisons involved different species as well as different mortality contexts. Within the *Delphinus delphis* dataset examined here, no consistent increase in cortical or medullary irregularities was detected across mortality categories, and overall glandular organization remained stable.

 doi:10.20944/preprints202603.1321.v1

Collectively, these observations indicate that adrenal morphology in *Delphinus delphis* is primarily shaped by species-specific structural patterns while retaining a degree of architectural flexibility.

4.2 Morphometry

Adrenal morphometry in *Delphinus delphis* demonstrated bilateral symmetry, with no consistent lateral differences in gland size or corticomedullary proportions. The corticomedullary ratio approximated unity in most individuals, indicating near-equivalent cortical and medullary thickness. This balanced organization contrasts with the more cortex-dominant patterns reported in other delphinids, including *Tursiops truncatus* and *Stenella* species [27,28], highlighting interspecific variability in adrenal proportional architecture within *Delphinidae*. Methodological differences may also contribute to variation among studies, as the present work employed standardized mid-transverse linear measurements, whereas others have used area-based or multivariate approaches [12,31].

Adrenal dimensions scaled proportionally to body length, supporting the interpretation that adrenal growth follows general somatic development [12,41,63]. Importantly, corticomedullary proportions differed significantly between immature and mature individuals, with mature dolphins exhibiting higher CM values overall. This pattern indicates ontogenetic reorganization of adrenal architecture during development. In contrast, maturity-related differences in corticomedullary ratio have not been reported in *Tursiops truncatus [27]*, further supporting species-specific developmental trajectories.

No consistent differences in corticomedullary ratio were detected between adult individuals who died from acute events and those who died following more progressive pathological processes. Although minor numerical variation was observed, distributions largely overlapped, indicating comparable corticomedullary architecture across mortality categories in this species. This contrasts with earlier observations in other dolphin species, in which bycaught individuals and those affected by chronic disease were reported to exhibit distinct adrenal proportional patterns [12,31].

Together, these findings suggest that adrenal proportional architecture may be influenced by species-specific and multifactorial physiological processes that extend beyond simple cause-of-death categorization. In cetaceans, cortical hyperplasia and adrenal enlargement have been described in association with chronic disease, contaminant exposure, and environmental stressors [14,31,64,65]. Similar patterns have been reported in other wildlife species exposed to prolonged anthropogenic or ecological pressures , and experimental models demonstrate that sustained ACTH stimulation or chronic stress paradigms can induce adrenocortical hypertrophy [66,67]. However, adrenal responses are not uniformly hypertrophic; cortical thinning, reduced adrenal mass, or zona-specific atrophy have also been documented under certain conditions [68,69]. In some models, sustained stress altered the HPA-axis sensitivity without consistent macroscopic enlargement [70–74], highlighting the complexity and context-dependence of endocrine–morphological relationships.

Accordingly, interpreting corticomedullary ratio as a direct structural proxy for chronic stress requires caution. Developmental stage, age-related remodeling, reproductive status, metabolic condition, and species-specific regulatory mechanisms may substantially influence adrenal proportional organization [75,76] The significant differences observed between immature and mature individuals in the present study further emphasize the impact of developmental stage on corticomedullary organisation.

While classification of mortality as “acute” or “chronic” provides a useful epidemiological framework, it may not fully capture the complexity of an individual’s endocrine history. Animals that die from sudden events may have experienced prior physiological challenges, whereas those assigned to chronic pathological categories may exhibit heterogeneous or fluctuating endocrine states. Within this intra-specific dataset, where age class and sexual maturity were explicitly considered, corticomedullary proportions in adult *Delphinus delphis* did not vary consistently between mortality categories. These findings suggest that, in this species, corticomedullary ratio

 doi:10.20944/preprints202603.1321.v1

appears more strongly influenced by developmental processes than by terminal pathological context, and its interpretation should consider broader biological and physiological context.

4.3. Ultrastructural Organization of the Adrenal Gland

Transmission electron microscopy confirmed that the adrenal gland of *Delphinus delphis* conforms broadly to the conserved mammalian ultrastructural framework, particularly in steroidogenic cortical organization and chromaffin cell architecture. Cells of the zona fasciculata exhibited abundant smooth endoplasmic reticulum, numerous mitochondria with tubular cristae, and prominent lipid droplets, consistent with the classical "spongiocyte" morphology described across mammals and associated with glucocorticoid biosynthesis [77–80]. Zona reticularis cells displayed comparatively greater cytoplasmic electron density and increased lysosomal components, features aligned with androgen precursor synthesis and terminal differentiation described in other vertebrate models [81], indicating preservation of core steroidogenic ultrastructural features within *Odontoceti.*

Within the adrenal medulla, two morphologically distinct chromaffin cell populations were identified based on secretory granule morphology and electron density. One population exhibited relatively homogeneous, electron-dense granules with narrow or poorly defined halos, whereas the second displayed pleomorphic granules with eccentrically located dense cores surrounded by a well-defined electron-lucent halo. This chromaffin granule heterogeneity corresponds to the classical ultrastructural distinction between epinephrine- and norepinephrine-producing chromaffin cells described in mammalian medullary studies [47,82,83]. Contemporary reviews continue to support granule morphology as a reliable ultrastructural correlate of catecholamine phenotype in the absence of immunohistochemical confirmation [56]. Although definitive functional assignment in *Delphinus delphis* would require direct immunolabeling, the granule characteristics observed here strongly support the presence of both catecholaminergic populations. Together, these observations confirm that adrenal ultrastructure in *Delphinus delphis* conforms to conserved mammalian organizational principles while contributing new species-level ultrastructural detail.

5. Conclusions

This study provides the first integrated gross, histological, morphometric, and ultrastructural characterization of the adrenal gland in Delphinus delphis. Adrenal architecture in this species conforms to conserved mammalian organizational principles while displaying species-specific structural patterns within Delphinidae.

Corticomedullary proportions were influenced by ontogenetic stage but did not vary consistently according to mortality category, highlighting the importance of developmental context in interpreting adrenal morphology. Ultrastructural findings confirmed preserved steroidogenic and catecholaminergic cellular organization, including distinct chromaffin cell populations.

Given the integrative and multifactorial regulation of the HPA axis, structural parameters should not be interpreted in isolation as direct indicators of stress or dysfunction. Rather, they should be considered within the broader context of species-specific organization, developmental dynamics, and physiological state. Continued investigation of adrenal morphology in conjunction with functional, endocrine, and comparative approaches will be essential to further elucidate the complex neuroendocrine regulation underlying stress responses in cetaceans.

By defining structural baselines for Delphinus delphis, this work establishes a reference framework for future comparative studies and for the evaluation of endocrine-related findings in health assessment and stranding investigations, promoting a biologically contextualized approach to adrenal assessment rather than reduction of structural variation to a single proxy of stress.

Supplementary Materials: The following supporting information can be downloaded at: Preprints.org, Table S1. Complete morphometric and histomorphometric dataset of Delphinus delphis included in the study; Table S2. Sexually mature Delphinus delphis included in cause-of-death comparative analyses

 doi:10.20944/preprints202603.1321.v1

;Figure S1. Absolute adrenal morphometry in sexually mature Delphinus delphis by sex; Figure S2. Comparison of corticomedullary ratio (CM) according to sexual maturity in Delphinus delphis; Figure S3. Comparison of corticomedullary ratio (CM) between acute and non-acute cause-of-death (COD) groups in sexually mature Delphinus delphis; Table S3. Mean diameter (nm) of mitochondria and lipid droplets in the adrenal cortex of Delphinus delphis; Table S4. Mean cell diameter (μm) of adrenal medullary cells in Delphinus delphis; Supplementary Document 1. Administrative authorization For the handling of stranded specimens on the Canary Islands coast, the collection and custody of their biological samples, and the performance of necropsies for scientific and conservation purposes

Author Contributions: Conceptualization, P.A.-A., and A.F.; methodology, P.A.-A.,and A.B.; software, I.M.-D., and D.L.R.; validation, A.F., A.B., M.A. and E.S.; formal analysis, P.A.-A., I.M.-D., A.F.,R.G.G.; investigation, P.A.-A., A.B.; resources, A.F., P.A., and M.A.; data curation, P.A.-A., R.G.G., and I.M.-D.; writing—original draft preparation, P.A.A.; writing—review and editing, P.A.-A., I.M.D., A.F., M.A., R.G.G., D.L.R., and A.B; visualization, P.A.-A. ; supervision, P.A.A., A.F; project administration M.A and A.F.; funding acquisition, PA.A. and A.F.. All authors have read and agreed to the published version of the manuscript.

Funding: The research that led to these findings was supported by a INPhINIT fellowship (Cohort 2022) from the "la Caixa" Foundation (ID 100010434), with the fellowship code "LCF/BQ/DR22/11950025"; as well as support from a National Research Project from the Spanish Ministry of Science, with the code "PID2021-127687NB-10".

Institutional Review Board Statement: Ethical review was not required for this study under the current Spanish legislation (Real Decreto 53/2013). No live animal experimentation occurred, samples for this study belonged to deceased specimens.

Data Availability Statement: The data on stranded animals and associated information are owned by the Canarian local government and are publicly available upon request. These data are held by the University of Las Palmas de Gran Canaria (ULPGC). Additional data generated and analyzed in this study may be available upon reasonable request..

Acknowledgments: The authors would like to thank the Canary Islands Cetacean Stranding Network for their support and collaboration throughout this study.

Conflicts of Interest: The authors declare no conflicts of interest. The funders had no role in the design of the study; in the collection, analyses, or interpretation of data; in the writing of the manuscript; or in the decision to publish the results.

Abbreviations

The following abbreviations are used in this manuscript:

HPA	Hypothalamic-pituitary-adrenal
CM	Corticomedullary
COD	Cause of death
TEM	Transmission electron microscopy
IUSA	Instituto Universitario de Sanidad Animal y Seguridad Alimentaria
ULPGC	Universidad de Las Palmas de Gran Canaria
HE	Hematoxylin-eosin
MT	Massons's trichrome
PAS	Periodic acid–Schiff
PAS-D	Periodic acid–Schiff-Diastase
IQR	Interquartile range
SD	Standard deviation
PBS	Phosphate-buffered saline
ZG	*Zona glomerulosa*
ZF	*Zona fasciculata*

 doi:10.20944/preprints202603.1321.v1

ZR	*Zona reticularis*
A	Adrenaline
NA	Noradrenaline

References

1. Vogt, M. The Role of the Adrenal Gland in Homeostasis. *Quarterly Journal of Experimental Physiology and Cognate Medical Sciences: Translation and Integration* **1954**, *39*, 245–252.
2. Silva, D. De; Journal, B.W.-C.M.; 2009, undefined The Adrenal Glands and Their Functions. *cmj.sljol.info*.
3. Peters, A.; Conrad, M.; Hubold, C.; Schweiger, U.; Fischer, B.; Fehm, H.L. The Principle of Homeostasis in the Hypothalamus-Pituitary-Adrenal System: New Insight from Positive Feedback. *American Journal of Physiology-Regulatory, Integrative and Comparative Physiology* **2007**, *293*, R83–R98.
4. Armario, A. The Hypothalamic-Pituitary-Adrenal Axis: What Can It Tell Us about Stressors? *CNS & Neurological Disorders-Drug Targets (Formerly Current Drug Targets-CNS & Neurological Disorders)* **2006**, *5*, 485–501.
5. Papadimitriou, A.; Priftis, K.N. Regulation of the Hypothalamic-Pituitary-Adrenal Axis. *Neuroimmunomodulation* **2009**, *16*, 265–271.
6. Harvey, S.; Phillips, J.G.; Rees, A.; Hall, T.R. Stress and Adrenal Function. *Wiley Online Library* **1984**, *232*, 633–645, doi:10.1002/jez.1402320332.
7. Möstl, E.; Palme, R. Hormones as Indicators of Stress. *Domest. Anim. Endocrinol.* **2002**, *23*, 67–74.
8. Ehrhart-Bornstein, M.; Bornstein, S.R. Stress Hormones and Immune Function. *Elsevier* **2008**, *1148*, 112–117, doi:10.1196/annals.1410.053.
9. Tsigos, C.; research, G.C.-J. of psychosomatic; 2002, undefined Hypothalamic–Pituitary–Adrenal Axis, Neuroendocrine Factors and Stress. *Elsevier*.
10. Burgess, E.; Hunt, K.; Kraus, S.; Comparative, R.R.-G. and; 2017, undefined Adrenal Responses of Large Whales: Integrating Fecal Aldosterone as a Complementary Biomarker to Glucocorticoids. *Elsevier*.
11. Pujade, L. Development of a Biomarker Panel for Identifying Stressed Marine Mammals. **2019**.
12. Medina Santana, C.; Slattery, O.; O'Donovan, J.; Murphy, S. Histological and Proteomic Approaches to Assessing the Adrenal Stress Response in Common Dolphins (Delphinus Delphis). *Animals* **2025**, *15*, doi:10.3390/ani15192924.
13. Burgess, E.A.; Hunt, K.E.; Kraus, S.D.; Rolland, R.M. Adrenal Responses of Large Whales: Integrating Fecal Aldosterone as a Complementary Biomarker to Glucocorticoids. *Gen. Comp. Endocrinol.* **2017**, *252*, 103–110.
14. Kuiken, T.; Höfle, U.; Bennett, P.M.; Allchin, C.R.; Kirkwood, J.K.; Baker, J.R.; Appleby, E.C.; Lockyer, C.H.; Walton, M.J.; Sheldrick, M.C. Adrenocortical Hyperplasia, Disease and Chlorinated Hydrocarbons in the Harbour Porpoise (Phocoena Phocoena). *Mar. Pollut. Bull.* **1993**, *26*, 440–446, doi:10.1016/0025-326X(93)90532-O.
15. St. Aubin, D.J.; Ridgway, S.H.; Wells, R.S.; Rhinehart, H. Dolphin Thyroid and Adrenal Hormones: Circulating Levels in Wild and Semidomesticated Tursiops Truncatus, and Influence of Sex, Age, and Season. *Mar. Mamm. Sci.* **1996**, *12*, 1–13, doi:10.1111/j.1748-7692.1996.tb00301.x.
16. Avisse, C.; Marcus, C.; Patey, M.; Ladam-Marcus, V.; Delattre, J.-F.; Flament, J.-B. Surgical Anatomy and Embryology of the Adrenal Glands. *Surgical Clinics of North America* **2000**, *80*, 403–415.
17. Zwemer, R.L. A Study of Adrenal Cortex Morphology. *Am. J. Pathol.* **1936**, *12*, 107.
18. Neville, A.M.; O'hare, M.J. Histopathology of the Human Adrenal Cortex. *Clin. Endocrinol. Metab.* **1985**, *14*, 791–820.
19. Gorgas, K.; Böck, P. Morphology and Histochemistry of the Adrenal Medulla: I. Various Types of Primary Catecholamine-Storing Cells in the Mouse Adrenal Medulla. *Histochemistry* **1976**, *50*, 17–31.
20. Siasios, A.; Delis, G.; Tsingotjidou, A.; Pourlis, A.; Grivas, I. Adrenal Glands of Mice and Rats: A Comparative Morphometric Study. *Lab. Anim.* **2022**, *56*, 247–258.
21. Milano, E.G.; Basari, F.; Chimenti, C. Adrenocortical and Adrenomedullary Homologs in Eight Species of Adult and Developing Teleosts: Morphology, Histology, and Immunohistochemistry. *Gen. Comp. Endocrinol.* **1997**, *108*, 483–496.

22. Barszcz, K.; Przespolewska, H.; Olbrych, K.; Czopowicz, M.; Klećkowska-Nawrot, J.; Goździewska-Harłajczuk, K.; Kupczyńska, M. The Morphology of the Adrenal Gland in the European Bison (Bison Bonasus). *Springer* **2016**, *12*, doi:10.1186/s12917-016-0783-8.
23. Zhongjie, L. The Adrenal Gland of Chinese River Dolphin (Lipotes Vexillifer). *Acta Hydrobiol. Sinica* **1988**, *12*, 59–64.
24. Bourne, G.H. The Mammalian Adrenal Gland. **1949**.
25. Jacobsen, A.P. *Endocrinological Studies in the Blue Whale:(Balaenoptera Musculus L.)*; I kommisjon hos Jacob Dybwad, 1941;
26. Vuković, S.; Lucić, H.; Živković, A.; Duras Gomerčić, M.; Gomerčić, T.; Galov, A. Histological Structure of the Adrenal Gland of the Bottlenose Dolphin (Tursiops Truncatus) and the Striped Dolphin (Stenella Coeruleoalba) from the Adriatic Sea. *Journal of Veterinary Medicine Series C: Anatomia Histologia Embryologia* **2010**, *39*, 59–66, doi:10.1111/j.1439-0264.2009.00981.x.
27. Clark, L.S.; Pfeiffer, D.C.; Cowan, D.F. Morphology and Histology of the Atlantic Bottlenose Dolphin (Tursiops Truncatus) Adrenal Gland with Emphasis on the Medulla. *Journal of Veterinary Medicine Series C: Anatomia Histologia Embryologia* **2005**, *34*, 132–140, doi:10.1111/J.1439-0264.2004.00600.X.
28. Clark, L.S.; Cowan, D.F.; Pfeiffer, D.C. A Morphological and Histological Examination of the Pan-Tropical Spotted Dolphin (Stenella Attenuata) and the Spinner Dolphin (Stenella Longirostris) Adrenal Gland. *Journal of Veterinary Medicine Series C: Anatomia Histologia Embryologia* **2008**, *37*, 153–159, doi:10.1111/J.1439-0264.2007.00821.X.
29. Carballeira, A.; Brown, J.W.; Fishman, L.M.; Trujillo, D.; Odell, D.K. The Adrenal Gland of Stranded Whales (Kogia Breviceps and Mesoplodon Europaeus): Morphology, Hormonal Contents, and Biosynthesis of Corticosteroids. *Gen. Comp. Endocrinol.* **1987**, *68*, 293–303.
30. Simpson, J.G.; Gardner, M.B. Comparative Microscopic Anatomy of Selected Marine Mammals. **1972**.
31. Clark, L.S.; Cowan, D.F.; Pfeiffer, D.C. Morphological Changes in the Atlantic Bottlenose Dolphin (Tursiops Truncatus) Adrenal Gland Associated with Chronic Stress. *J. Comp. Pathol.* **2006**, *135*, 208–216, doi:10.1016/j.jcpa.2006.07.005.
32. Jefferson, T.A.; Fertl, D.; Bolaños-Jiménez, J.; Zerbini, A.N. Distribution of Common Dolphins (Delphinus Spp.) in the Western Atlantic Ocean: A Critical Re-Examination. *Marine Biology 2009 156:6* **2009**, *156*, 1109–1124, doi:10.1007/s00227-009-1152-y.
33. Selzer, L.A.; Payne, P.M. The Distribution of White-Sided (Lagenorhynchus Acutus) and Common Dolphins (Delphinus Delphis) Vs. Environmental Features of the Continental Shelf of the Northeastern United States. *Mar. Mamm. Sci.* **1988**, *4*, 141–153, doi:10.1111/j.1748-7692.1988.tb00194.x.
34. Vuković, S.; Lucić, H.; Đuras Gomerčić, M.; Galov, A.; Gomerčić, T.; Ćurković, S.; Škrtić, D.; Domitran, G.; Gomerčić, H. Anatomical and Histological Characteristics of the Pituitary Gland in the Bottlenose Dolphin (*Tursiops Truncatus*) from the Adriatic Sea. *the Adriatic Sea.. Vet. arhiv* **2011**, *81*, 143–151.
35. Alonso-Almorox, P.; Blanco, A.; Fiorito, C.; Gómez-Villamandos, J.C.; Risalde, M.A.; Almunia, J.; Fernández, A. The Orca (Orcinus Orca) Pituitary Gland: An Anatomical, Immunohistochemical and Ultrastructural Analysis. *Frontiers in Neuroanatomy* **2025**, *19*, 1626079, doi:10.3389/FNANA.2025.1626079/BIBTEX.
36. Alonso-Almorox, P.; Blanco, A.; Fiorito, C.; Sierra, E.; Suárez-Santana, C.; Consolli, F.; Arbelo, M.; Guzmán, R.G.; Molpeceres-Diego, I.; Fernández Gómez, A.; et al. Dolphin Pituitary Gland: Immunohistochemistry and Ultrastructural Cell Characterization Following a Novel Anatomical Dissection Protocol and Non-Invasive Imaging (MRI). *Animals* **2025**, *15*, 735, doi:10.3390/ANI15050735/S1.
37. Kuiken, T.; García-Hartmann, M. Proceedings of the First European Cetacean Society Workshop on Cetacean Pathology: Dissection Techniques and Tissue Sampling. In Proceedings of the ECS Workshop on Cetacean Pathology; 1991; p. 20.
38. Reynolds, J.E., S.A.R. and M.E.B. *Anatomical Dissection: Thorax and Abdomen. In: Encyclopedia of Marine Mammals*; Academic Press: San Diego, 2002;
39. Rommel, S.A.; L. J. Lowenstine Gross and Microscopic Anatomy. In: CRC Hanbook of Marine Mammal Medicine 2001.

 doi:10.20944/preprints202603.1321.v1

40. Jelinek, F.; Konecny, R. Adrenal Glands of Slaughtered Bulls, Heifers and Cows: A Histological Study. *Journal of Veterinary Medicine Series C: Anatomia Histologia Embryologia* **2011**, *40*, 28–34, doi:10.1111/j.1439-0264.2010.01034.x.
41. Cowan, D.F. Observations on the Pilot Whale Globicephala Melaena: Organweight and Growth. *Anat. Rec.* **1966**, *155*, 623–628, doi:10.1002/ar.1091550413.
42. Nicolaides, N.C.; Willenberg, H.S.; Bornstein, S.R.; Chrousos, G.P. Adrenal Cortex: Embryonic Development, Anatomy, Histology and Physiology. *Endotext* **2023**.
43. Neville, A.; metabolism, M.O.-C. in endocrinology and; 1985, undefined Histopathology of the Human Adrenal Cortex. *Elsevier*.
44. Anderson, J.; journal, A.R.-P. medical; 1980, undefined Ectopic Adrenal Tissue in Adults. *pmc.ncbi.nlm.nih.govJR Anderson, AHML RossPostgraduate medical journal, 1980•pmc.ncbi.nlm.nih.gov*.
45. Schmidt, M.; Enthoven, L.; … M.V.D.M.-I. journal of; 2003, undefined The Postnatal Development of the Hypothalamic–Pituitary–Adrenal Axis in the Mouse. *Elsevier*, doi:10.1016/S0736-5748.
46. Fenwick, E.; Fajdiga, P.; … N.H.-T.J. of cell; 1978, undefined Functional and Morphological Characterization of Isolated Bovine Adrenal Medullary Cells. *rupress.orgEM Fenwick, PB Fajdiga, NB Howe, BG LivettThe Journal of cell biology, 1978•rupress.org*.
47. Coupland, R.; Anatomy, B.W.-J. of; 1970, undefined Electron Microscopic Observation on the Adrenal Medulla and Extra-Adrenal Chromaffin Tissue of the Postnatal Rabbit. *pmc.ncbi.nlm.nih.govRE Coupland, BS WeakleyJournal of Anatomy, 1970•pmc.ncbi.nlm.nih.gov*.
48. Coupland, R.E. Electron Microscopic Observations on the Structure of the Rat Adrenal Medulla: I. The Ultrastructure and Organization of Chromaffin Cells in the Normal Adrenal Medulla. *J. Anat.* **1965**, *99*, 231.
49. Bornstein, S.R.; Gonzalez-Hernandez, J.A.; Ehrhart-Bornstein, M.; Adler, G.; Scherbaum, W.A. Intimate Contact of Chromaffin and Cortical Cells within the Human Adrenal Gland Forms the Cellular Basis for Important Intraadrenal Interactions. *J. Clin. Endocrinol. Metab.* **1994**, *78*, 225–232, doi:10.1210/jcem.78.1.7507122.
50. Bornstein, S.R.; Ehrhart-Bornstein, M.; Scherbaum, W.A. Morphological and Functional Studies of the Paracrine Interaction between Cortex and Medulla in the Adrenal Gland. *Microsc. Res. Tech.* **1997**, *36*, 520–533.
51. Mitani, F.; Suzuki, H.; Hata, J.; … T.O.-; 1994, undefined A Novel Cell Layer without Corticosteroid-Synthesizing Enzymes in Rat Adrenal Cortex: Histochemical Detection and Possible Physiological Role. *academic.oup.com*.
52. Teixeira, B.; Zoology, M.& K.-A.; 1993, undefined The Adrenal Gland of the African Buffalo, Syncerus Caffer: A Light and Electron Microscopic Study. *journals.co.za*, doi:10.10520/AJA00445096_504.
53. Gbadebo Olukole, S.; Abosede Adeagbo, M.; Olusiji Oke, B.; Histology, B.O. Histology and Histochemistry of the Adrenal Gland African Giant Rat (Cricetomys Gambianus, Waterhouse). *pdfs.semanticscholar.org* **2016**, *34*, 1455–1460.
54. Neville, A.; O'Hare, M. The Human Adrenal Cortex: Pathology and Biology—an Integrated Approach. **2012**.
55. Weiss, C.; Cahill, A.; Laslop, A.; … R.F.-C.-N.; 1996, undefined Differences in the Composition of Chromaffin Granules in Adrenaline and Noradrenaline Containing Cells of Bovine Adrenal Medulla. *Elsevier*.
56. Carbone, E.; Borges, R.; Eiden, L.E.; García, A.G.; Hernández-Cruz, A. Chromaffin Cells of the Adrenal Medulla: Physiology, Pharmacology, and Disease. *Wiley Online Library* **2019**, *9*, 1443–1502, doi:10.1002/j.2040-4603.2019.tb00098.x.
57. Paul, B., S.S., I.M.N., & D.R. Morphological and Histological Investigations on the Adrenal Glands in Black Bengal Goat (Capra Hircus). *Journal of the Sylhet Agricultural University* **2016**, *3*, 181–187.
58. Nicolaides, N.C.; Willenberg, H.S.; Bornstein, S.R.; Chrousos, G.P. Adrenal Cortex: Embryonic Development, Anatomy, Histology and Physiology. *Endotext* **2023**.
59. Abdellatif, A.B.; Fernandes-Rosa, F.L.; Boulkroun, S.; Zennaro, M.C. Vascular and Hormonal Interactions in the Adrenal Gland. *Front. Endocrinol. (Lausanne).* **2022**, *13*, 995228, doi:10.3389/fendo.2022.995228.

 doi:10.20944/preprints202603.1321.v1

60. Gomez-Sanchez, C.E. Regulation of Adrenal Arterial Tone by Adrenocorticotropin: The Plot Thickens. *Endocrinology* **2007**, *148*, 3566–3568, doi:10.1210/en.2007-0560.
61. Vinson, G.P.; Pudney, J.A.; Whitehouse, B.J. The Mammalian Adrenal Circulation and the Relationship between Adrenal Blood Flow and Steroidogenesis.
62. Breed, D.; Meyer, L.C.R.; Steyl, J.C.A.; Goddard, A.; Burroughs, R.; Kohn, T.A. Conserving Wildlife in a Changing World: Understanding Capture Myopathy—a Malignant Outcome of Stress during Capture and Translocation. *Conserv. Physiol.* **2019**, *7*, doi:10.1093/conphys/coz027.
63. Turner, J.; Clark, L.; Haubold, E.; … G.W.-A.; 2006, undefined Organ Weights and Growth Profiles in Bottlenose Dolphins (Tursiops Truncatus) from the Northwestern Gulf of Mexico. *academia.eduJP Turner, LS Clark, EM Haubold, GAJ Worthy, DF CowanAquatic Mammals, 2006•academia.edu*.
64. Venn-Watson, S.; Colegrove, K.M.; Litz, J.; Kinsel, M.; Terio, K.; Saliki, J.; Fire, S.; Carmichael, R.; Chevis, C.; Hatchett, W.; et al. Adrenal Gland and Lung Lesions in Gulf of Mexico Common Bottlenose Dolphins (Tursiops Truncatus) Found Dead Following the Deepwater Horizon Oil Spill. *PLoS One* **2015**, *10*, doi:10.1371/journal.pone.0126538.
65. Lair, S.; Béland, P.; De Guise, S.; Martineau, D. Adrenal Hyperplastic and Degenerative Changes in Beluga Whales. *J. Wildl. Dis.* **1997**, *33*, 430–437, doi:10.7589/0090-3558-33.3.430.
66. Martí, O.; Gavaldà, A.; Jolín, T.; Armario, A. Effect of Regularity of Exposure to Chronic Immobilization Stress on the Circadian Pattern of Pituitary Adrenal Hormones, Growth Hormone, and Thyroid Stimulating Hormone in the Adult Male Rat. *Psychoneuroendocrinology* **1993**, *18*, 67–77, doi:10.1016/0306-4530(93)90056-Q.
67. Ulrich-Lai, Y.M.; Figueiredo, H.F.; Ostrander, M.M.; Choi, D.C.; Engeland, W.C.; Herman, J.P. Chronic Stress Induces Adrenal Hyperplasia and Hypertrophy in a Subregion-Specific Manner. *https://doi.org/10.1152/ajpendo.00070.2006* **2006**, *291*, 965–973, doi:10.1152/ajpendo.00070.2006.
68. Koko, V.; Djordjeviæ, J.; Cvijiæ, G.; Davidoviæ, V. Effect of Acute Heat Stress on Rat Adrenal Glands: A Morphological and Stereological Study. *Journal of Experimental Biology* **2004**, *207*, 4225–4230, doi:10.1242/jeb.01280.
69. Berger, I.; Werdermann, M.; Bornstein, S.R.; Steenblock, C. The Adrenal Gland in Stress – Adaptation on a Cellular Level. *J. Steroid Biochem. Mol. Biol.* **2019**, *190*, 198–206, doi:10.1016/j.jsbmb.2019.04.006.
70. Spencer, K.A. Developmental Stress and Social Phenotypes: Integrating Neuroendocrine, Behavioural and Evolutionary Perspectives. *Philosophical Transactions of the Royal Society B: Biological Sciences* **2017**, *372*, doi:10.1098/rstb.2016.0242.
71. DeRijk, R.; De Kloet, E.R. Corticosteroid Receptor Genetic Polymorphisms and Stress Responsivity. *Endocrine 2005 28:3* **2005**, *28*, 263–269, doi:10.1385/ENDO:28:3:263.
72. Charmandari, E. Primary Generalized Glucocorticoid Resistance and Hypersensitivity: The End-Organ Involvement in the Stress Response. *Sci. Signal.* **2012**, *5*, doi:10.1126/scisignal.2003337.
73. Kinlein, S.; neuroendocrinology, I.K.-F. in; 2020, undefined The Hypothalamic-Pituitary-Adrenal Axis as a Substrate for Stress Resilience: Interactions with the Circadian Clock. *Elsevier*.
74. Herman, J.P.; McKlveen, J.M.; Ghosal, S.; Kopp, B.; Wulsin, A.; Makinson, R.; Scheimann, J.; Myers, B. Regulation of the Hypothalamic-pituitary-adrenocortical Stress Response. *Wiley Online LibraryJP Herman, JM McKlveen, S Ghosal, B Kopp, A Wulsin, R Makinson, J Scheimann, B MyersComprehensive physiology, 2016•Wiley Online Library* **2016**, *6*, 603–621, doi:10.1002/j.2040-4603.2016.tb00694.x.
75. Yiallouris, A.; Filippou, C.; Themistocleous, S.C.; Menelaou, K.; Kalodimou, V.; Michaeloudes, C.; Johnson, E.O. Aging of the Adrenal Gland and Its Impact on the Stress Response. *Vitam. Horm.* **2024**, *124*, 341–366, doi:10.1016/bs.vh.2023.12.004.
76. Li, N.; Li, Y.; Lu, Y.; Zhang, K.; Wang, S.; Wang, C. The Impact of Chronic Stress on Cortical Thickness in Patients with Depression. *Front. Psychiatry* **2025**, *16*, 1554476, doi:10.3389/fpsyt.2025.1554476.
77. Ishimura, K.; technique, H.F.-M. research and; 1997, undefined Light and Electron Microscopic Immunohistochemistry of the Localization of Adrenal Steroidogenic Enzymes. *Wiley Online Library*, doi:10.1002/(SICI).
78. Japonica, A.K.-A.P.; 1969, undefined Ultrastructural Zonation of the Human Adrenal Cortex. *Wiley Online Library* **1969**, *19*, 115–149, doi:10.1111/j.1440-1827.1969.tb00698.x.

 doi:10.20944/preprints202603.1321.v1

79. Pathologie, E.M.-B. zur; 1974, undefined Ultrastructure and Function of the Mesenchyme of the Rat Adrenal Cortex. *Elsevier*.
80. Dickens, R. An Ultrastructural and Morphometric Study of the Adrenal Cortex in the Intact and Hypophysectomized Male Rat. **1975**.
81. Pihlajoki, M.; Dörner, J.; Cochran, R.S.; Heikinheimo, M.; Wilson, D.B. Adrenocortical Zonation, Renewal, and Remodeling. *Front. Endocrinol. (Lausanne).* **2015**, *6*, 131775, doi:10.3389/fendo.2015.00027.
82. Carmichael, S.; American, H.W.-S.; 1985, undefined The Adrenal Chromaffin Cell. *JSTORSW Carmichael, H WinklerScientific American, 1985•JSTOR*.
83. Neurosciences, H.W.-C. in the; 1980, undefined The Composition of Adrenal Chromaffin Granules: An Assessment of Controversial Results. *Elsevier*.